

CrossMark  
click for updatesCite this: *J. Mater. Chem. A*, 2016, 4, 17604Received 15th August 2016  
Accepted 10th October 2016

DOI: 10.1039/c6ta06978a

www.rsc.org/MaterialsA

## Non-fullerene small molecule acceptors based on perylene diimides

Zhitian Liu, Yao Wu, Qi Zhang and Xiang Gao\*

Great advances in the subfield of non-fullerene acceptors have been achieved in the last few years. Perylene diimides are among the most investigated due to their excellent electron mobility, high electron affinity and feasible chemical modification. In this review, we summarize reports of small molecule acceptors based on perylene diimides in recent years and highlight the effect of molecular structure on their performance in bulk heterojunction organic solar cells with the hope of providing criteria for designing acceptors based on perylene diimides.

### 1. Introduction

Bulk heterojunction (BHJ) organic solar cells (OSCs) have been widely investigated for their light weight, short payback time, and the capability to fabricate flexible devices.<sup>1–9</sup> The typical BHJ blend films consist of polymer donor materials and fullerene acceptor materials.<sup>10–12</sup> Great advances in developing high efficiency polymer donor materials have been achieved.<sup>13</sup> Fullerene and its derivatives are still the most popular electron acceptors because they exhibit strong electron affinity, high electron mobility, and ultrafast photo-induced charge transfer and charge separation.<sup>14</sup> However, fullerene and its derivatives are too expensive for large-scale production and it is difficult to modify their chemical structure.<sup>12,15</sup> During the last few years

many efforts have been made to design and synthesize non-fullerene acceptors.<sup>16,17</sup> Some new non-fullerene acceptors (NFAs) have shown potential to outperform fullerenes in comparative devices.<sup>18–22</sup> To date, maximum power conversion efficiency (PCE) of BHJ OSCs based on NFAs over 12% has been reported.<sup>23</sup> Research papers<sup>21,23–27</sup> and a review<sup>28</sup> are recommended for better understanding this kind of high efficiency fused-ring NFAs. Among the vast library of non-fullerene acceptors, perylene diimide (PDI) derivatives are also widely investigated due to their good electron-accepting ability, high electron mobility, especially various feasible methods to modify the frontier molecular orbital levels.<sup>29–34</sup> However, it appears rather surprising that the utilization of PDIs in OSCs is still lagging behind fullerenes. This can be attributed to that PDI based acceptors are inclined to aggregate in large size in BHJ active layers due to their strong  $\pi$ - $\pi$  stacking tendency.<sup>4</sup> The micrometer-sized crystallite, namely, micrometer-sized domain

School of Material Science & Engineering, Wuhan Institute of Technology, Wuhan 430073, PR China. E-mail: gaoliang@hust.edu.cn



Zhitian Liu is a full professor of materials science and engineering at Wuhan Institute of Technology. He specializes in the design, synthesis, and characterization of novel conjugated polymers and their application in novel optoelectronic devices. His current research activities focus on optoelectronic materials and devices, including light-emitting diodes and solar cells. He received his Ph.D.

degree in polymer materials from South China University of Technology under the guidance of Prof. Yong Cao and then worked as a visiting scholar in materials science and engineering at the University of California, Los Angeles with Prof. Qibing Pei.



Yao Wu obtained her bachelors degree at the Wuhan Institute of Technology, Hubei, China. Now she is currently a masters student working under the direction of Prof. Zhitian Liu and Dr Xiang Gao at the School of Materials and Engineering in Wuhan Institute of Technology. Her research is focused on the synthesis and characterization of novel non-fullerene acceptors based on perylene diimides.

inhibits charge separation at the donor/acceptor interface.<sup>9</sup> Since the diffusion length of excitons is only 5–20 nm,<sup>31,35</sup> moderate phase separation plays a vital role in achieving high efficiency. Besides, large aggregates facilitate excimer formation which traps excitons and thereby limits the diffusion length in PDIs and causes terminal loss of photo-induced excitons.<sup>32,36</sup>

To solve this problem, disrupting the planarity of PDIs has been proved to be a useful way to suppress the aggregation and enhance the photovoltaic performances. However, a decline in electron mobility usually comes with a twisted configuration. Since device performance depends largely on the charge-transport properties,<sup>37,38</sup> it is important to suppress the aggregation while preserving high electron mobility. Besides, the modulation of photoelectric properties should also be taken into account when a new acceptor is designed.<sup>39</sup> There are three functionalization positions in the PDI moiety: bay positions (1,6,7,12-positions), *ortho* positions (2,5,8,11-positions) and imide positions, as shown in Fig. 1. All of them can be used to construct the twisted configuration. (1) Functionalization at the bay position is a facile synthesis route to tune the optical and electronic properties and it is the easiest method to minimize the aggregation of PDI derivatives.<sup>34</sup> Monobrominated or dibrominated perylene diimide is usually used as the initial raw material. With the help of large steric substituents at the bay position or formation of PDI dimers, aggregation can be effectively suppressed. (2) Functionalization at imide positions is not as effective as functionalization

at the bay position to adjust the optical and electric properties because there are nodes at the imide nitrogen positions.<sup>26</sup> But substituents at imide positions will not lead to distortion of the PDI core and thus maintain intermolecular interactions in the solid state while the non-planar conformation between the PDI core and substituents suppresses the intrinsic  $\pi$ - $\pi$  stacking of PDIs in films. (3) Functionalization at the *ortho* position opens a new route to tune the properties of PDI effectively without disturbing the planarity of the perylene core, which combines a planar core and variable substituents with tunable properties and is considered as the most promising position to modify PDIs.<sup>32</sup> (4) Another effective strategy to reduce aggregation is to construct a fused nonplanar configuration. It inhibits the rotation of the single bond and enhances the solid order for improving charge mobility, while maintaining a nonplanar structure to suppress aggregates.<sup>40,41</sup> However, it is less investigated due to the relatively complicated synthesis route. Every method has its unique superiority and it is feasible to combine two or more methods to achieve optimal molecular geometry with desirable optical and electronic properties.

There is growing attention in developing non-fullerene acceptors in BHJ solar cells. This review focuses on small molecular NFAs based on perylene diimides with regard to not only remarkable high PCEs as described in other reviews, but also the development and optimization processes. The relationships between chemical molecular structures and energy levels, aggregation behaviors and the mobility are discussed, as well as the relationship between molecular geometry and OSC performances. This review probably sheds light on designing novel high efficiency acceptors based on perylene diimides. In order to make this review more readable, the structures of donor materials mentioned are drawn in Fig. 8 and the significant parameters of the acceptors are listed in Table 1.

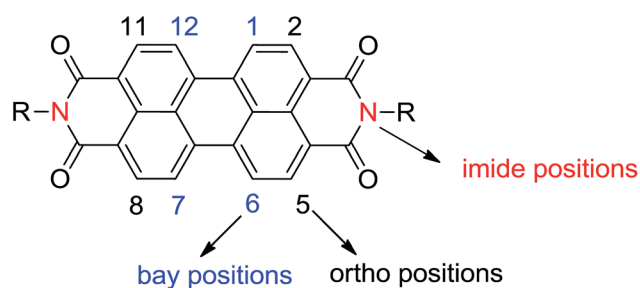


Fig. 1 Perylene diimide.

## 2. Bay positions

Modifying PDI *via* the bay position is the most investigated way to functionalize PDI due to synthesis feasibility which has been



Qi Zhang is a lecturer in the School of Materials Science and Engineering, Wuhan Institute of Technology. He received his B.S. degree in Wuhan Institute of Technology in 2004. He received his Ph.D. degree from School of Chemistry and Molecular Sciences, Wuhan University under the supervision of Prof. Zhinong Gao in 2012. His research interests include optoelectronic materials and molecular self-assembly.



Xiang Gao is a lecturer in the School of Materials Science & Engineering, Wuhan Institute of Technology. He received his B.S. degree (2009) in the School of Chemistry and Chemical Engineering, Huazhong University of Science and Technology and Ph.D. degree (2014) from Wuhan National Laboratory for Optoelectronics, Huazhong University of Science and Technology under the supervision of Prof.

Bin Hu and Prof. Guoli Tu. His research interests include synthesis of optoelectronic materials and their application in organic light-emitting diodes and organic solar cells.

Table 1 PV performances of acceptors based on PDIs

Acceptors	LUMO <sup>a</sup> (eV)	HOMO <sup>b</sup> (eV)	Donors	PCE <sup>c</sup> (%)	V <sub>oc</sub> (V)	J <sub>sc</sub> (mA cm <sup>-2</sup> )	FF (%)	μ <sub>e</sub> <sup>d</sup> (cm <sup>2</sup> V <sup>-1</sup> s <sup>-1</sup> )	Device architecture	D/A	Additive	Ref.
2.1a	-3.78(C)	-5.93(C)	P3HT	0.005	0.44	0.02	53	6.71 × 10 <sup>-2</sup> (S,B)	ITO/PEDOT:PSS/BHJ/Ca/Al	1:1.2	4% DIO	42
2.1b	-3.81(C)	-5.68(C)	P3HT	0.44	0.56	1.7	45	8.30 × 10 <sup>-7</sup> (S,B)	ITO/ZnO/BHJ/MnOx/Al	1:1.2	4% DIO	42
2.1c	-3.95(C)	-5.57(C)	P3HT	1.66	0.61	5.3	51	1.96 × 10 <sup>-5</sup> (S,B)	ITO/ZnO/BHJ/MnOx/Al	1:1.2	4% DIO	42
2.2	-3.82(C)	-5.69(C)	PTB7-Th	4.1	0.87	10.1	46.4	—	ITO/ZnO/BHJ/MnOx/Al	1:1.1	1% CN	43
2.3a	-4.09(C)	-6.09(L)	P3HT	0.82	0.65	1.96	64	8.79 × 10 <sup>-6</sup> (S,B)	ITO/ZnO/BHJ/MoO <sub>3</sub> /Al	1:1.1	2% DIO	45
2.3b	-4.08(C)	-6.14(L)	P3HT	1.12	0.68	2.88	57	8.51 × 10 <sup>-5</sup> (S,B)	ITO/ZnO/BHJ/MoO <sub>3</sub> /Al	1:1.1	2% DIO	45
2.3c	-4.08(C)	-6.19(L)	P3HT	0.72	0.64	2.03	55	4.98 × 10 <sup>-7</sup> (S,B)	ITO/ZnO/BHJ/MoO <sub>3</sub> /Al	1:1.1	2% DIO	45
2.3d	-4.07(C)	-6.10(L)	P3HT	0.77	0.63	1.93	63	—	ITO/ZnO/BHJ/MoO <sub>3</sub> /Al	1:1.1	2% DIO	46
2.3e	-4.06(C)	-6.08(L)	P3HT	0.38	0.65	1.03	56	—	ITO/ZnO/BHJ/MoO <sub>3</sub> /Al	1:1.1	2% DIO	46
2.3f	-4.06(C)	-6.09(L)	P3HT	0.4	0.65	1.52	40	4.64 × 10 <sup>-6</sup> (S,B)	ITO/ZnO/BHJ/MoO <sub>3</sub> /Al	1:1.1	1% DIO	46
3.1a	-3.87(C)	-5.95(C)	PBDTTP-C-T	3.63	0.73	10.58	46.8	—	ITO/PEDOT:PSS/BHJ/Ca/Al	1:1.1	1.5% DIO & 1.5% CN	47
3.1a	-3.87(C)	-5.95(C)	PBDTBD	4.39	0.87	8.26	61.1	—	ITO/PEDOT:PSS/BHJ/Ca/Al	1:1.1	1.5% DIO & 1.5% CN	48
3.1a	-4.04(C)	-6.13(C)	PBDTTP-F-TT	5.9	0.81	12.32	60	3.32 × 10 <sup>-5</sup> (S,B)	ITO/ZnO/BHJ/MoO <sub>3</sub> /Ag	1:1.1	1% DIO & 2% CN	49
3.1a	-4.28(C)	-6.35(L)	PDPPT2z2T	0.1	0.93	0.31	35	—	ITO/ZnO/BHJ/MoO <sub>3</sub> /Ag	1:1.1	0.2% DIO	58
3.1a	-3.75(C)	-5.81(C)	PTB7-Th	5.56	0.79	12.86	54	9.4 × 10 <sup>-5</sup> (S,B)	ITO/ZnO/BHJ/MoO <sub>3</sub> /Ag	1:1.1	1% DIO & 2% CN	53
3.1a	-3.87(C)	-5.95(C)	PBDTTPD	3.37	1.04	6.8	47.6	2.0 × 10 <sup>-4</sup> (S,B)	ITO/PEDOT:PSS/BHJ/Ca/Al	1:1.1	—	50
3.1a	-3.87(C)	-5.95(C)	PBDTTP-EFT	4.48	0.77	11.5	50.6	2.0 × 10 <sup>-4</sup> (S,B)	ITO/PEDOT:PSS/BHJ/Ca/Al	1:1.1	—	50
3.1a	-3.87(C)	-5.95(C)	PSBTBT	1.67	0.68	6.4	38.4	2.0 × 10 <sup>-4</sup> (S,B)	ITO/PEDOT:PSS/BHJ/Ca/Al	1:1.1	—	50
3.1a	-3.87(C)	-5.95(C)	PDPPT3T	0.98	0.71	3.5	40.3	2.0 × 10 <sup>-4</sup> (S,B)	ITO/PEDOT:PSS/BHJ/Ca/Al	2:1.1	—	50
3.1b	-3.96(H)	-5.99(C)	PfBT4T-2DT	5.4	0.84	11.4	53	7.8 × 10 <sup>-5</sup> (S,B)	ITO/ZnO/BHJ/V <sub>2</sub> O <sub>5</sub> /Al	1:1.4	No additive	84
3.1b	-3.73(C)	-6.21(C)	P3TEA	7.0	0.954	12.46	59.1	—	ITO/ZnO/BHJ/V <sub>2</sub> O <sub>5</sub> /Al	1:1.5	2.5% ODT	19
3.1c	-4.56(C)	-6.59(L)	PDPPT2z2T	1.4	0.77	5.5	34	—	ITO/ZnO/BHJ/MoO <sub>3</sub> /Ag	1:1.1	0.2% DIO	58
3.2a	-4.02(C)	-5.95(C)	PTB7-Th	3.65	0.88	9.74	41	5.85 × 10 <sup>-7</sup> (S,B)	ITO/ZnO/BHJ/MoO <sub>3</sub> /Ag	1:1.2	No additive	41
3.2b	-3.95(C)	-5.83(C)	P3HT	0.41	0.43	2.01	47.2	1.2 × 10 <sup>-3</sup> (S,B)	ITO/PEDOT:PSS/BHJ/Ca/Al	1:1.1	3% CN	73
3.2b	-3.95(C)	-5.83(C)	p-DTS(FBTTh <sub>2</sub> ) <sub>2</sub>	3.7	0.74	7.54	66.1	4.6 × 10 <sup>-4</sup> (S,B)	ITO/PEDOT:PSS/BHJ/Ca/Al	3:1.1	0.15% DIO	68
3.2c	-3.84(C)	-5.65(C)	PBDTTP-C-T	4.34	0.78	9.99	52.8	1.2 × 10 <sup>-3</sup> (S,B)	ITO/ZnO/BHJ/MnOx/Ag	1:1.1	2% DIO	57
3.2c	-3.84(C)	-5.65(C)	PBD-TTP-C-T	3.28	0.80	8.18	47.6	6.3 × 10 <sup>-4</sup> (S,B)	ITO/PEDOT:PSS/BHJ/Ca/Al	1:1.1	7% DIO	57
3.2d	-3.84(C)	-5.65(C)	PBDTTP-C-T	4.03	0.85	8.86	54.1	3.9 × 10 <sup>-3</sup> (O,N)	ITO/PEDOT:PSS/BHJ/Ca/Al	1:1.1	5% DIO	59
3.2d	-3.84(C)	-5.65(C)	PBDTTP-C-T	6.08	0.84	12.83	56.43	6.06 × 10 <sup>-3</sup> (S,B)	ITO/PEDOT:PSS/BHJ/Ca/Al	1:1.1	1.50% DIO	64
3.2d	-3.84(C)	-5.65(C)	PBDT-TS1	7.24	0.89	13.23	59.4	1.87 × 10 <sup>-4</sup> (S,B)	ITO/PEDOT:PSS/BHJ/PDINO/Al	1:1.5	3% DIO	65
3.2d	-3.84(C)	-5.65(C)	P3HT	0.76	0.59	2.89	44.8	4.1 × 10 <sup>-4</sup> (S,B)	ITO/PEDOT:PSS/BHJ/Ca/Al	1:1.1	8% CN	73
3.2e	-3.84(C)	-5.57(C)	P3HT	1.54	0.67	3.83	60.0	7.1 × 10 <sup>-4</sup> (S,B)	ITO/PEDOT:PSS/BHJ/Ca/Al	1:1.1	1.75% CN	73
P0TP	-3.84(C)	-5.74(C)	PBDTTP-C-T	0.76	0.84	2.11	42.7	7 × 10 <sup>-6</sup> (S,B)	ITO/PEDOT:PSS/BHJ/Ca/Al	1:1.1	3% DIO	63
P1TP	-3.72(C)	-5.66(C)	PBDTTP-C-T	3.61	0.89	7.78	52.1	2.4 × 10 <sup>-4</sup> (S,B)	ITO/PEDOT:PSS/BHJ/Ca/Al	1:1.1	3% DIO	63
P1TP	-3.86(C)	5.65(C)	PBDT-TS1	6.36	0.89	12.28	58.17	5.2 × 10 <sup>-5</sup> (O,N)	ITO/PEDOT:PSS/BHJ/PDINO/Al	1:1.1	2% DIO	66
P2TP	-3.76(C)	-5.63(C)	PBDTTP-C-T	0.79	0.83	3.05	31.3	1.2 × 10 <sup>-4</sup> (S,B)	ITO/PEDOT:PSS/BHJ/Ca/Al	1:1.1	2% DIO	63
P3TP	-3.75(C)	-5.61(C)	PBDTTP-C-T	0.91	0.77	3.38	35.0	4 × 10 <sup>-5</sup> (S,B)	ITO/PEDOT:PSS/BHJ/Ca/Al	1:1.1	3% DIO	63
Bis-PDI-1T-EG	-3.84(C)	-5.65(C)	P3HT	1.16	0.57	3.18	64.3	7.2 × 10 <sup>-4</sup> (S,B)	ITO/PEDOT:PSS/BHJ/Ca/Al	1:1.1	No additive	74
Bis-PDI-1T-EG	-3.84(C)	-5.65(C)	DPP-BDT-T	1.62	0.83	3.79	51	2.3 × 10 <sup>-5</sup> (S,B)	ITO/PEDOT:PSS/BHJ/Ca/Al	1:1.1	2% DIO	67
Bis-PDI-2T-EG	-3.84(C)	-5.54(C)	P3HT	0.38	0.64	1.15	52.6	1.5 × 10 <sup>-4</sup> (S,B)	ITO/PEDOT:PSS/BHJ/Ca/Al	1:1.1	No additive	74
Bis-PDI-3T-EG	-3.84(C)	-5.36(C)	P3HT	0.25	0.38	1.50	44.4	5.3 × 10 <sup>-5</sup> (S,B)	ITO/PEDOT:PSS/BHJ/Ca/Al	1:1.1	No additive	74
Bis-PDI-4T-EG	-3.84(C)	-5.24(C)	P3HT	1.08	0.66	2.76	59.7	5.7 × 10 <sup>-4</sup> (S,B)	ITO/PEDOT:PSS/BHJ/Ca/Al	1:1.1	No additive	74
Bis-PDI-5T-EG	-3.84(C)	-5.23(C)	P3HT	0.11	0.51	0.66	32.5	1.7 × 10 <sup>-5</sup> (S,B)	ITO/PEDOT:PSS/BHJ/Ca/Al	1:1.1	No additive	74
Bis-PDI-6T-EG	-3.84(C)	-5.10(C)	P3HT	1.26	0.62	4.57	44.2	3.9 × 10 <sup>-4</sup> (S,B)	ITO/PEDOT:PSS/BHJ/Ca/Al	1:1.1	No additive	74
3.3a	-3.85(C)	-5.80(C)	PTB7-Th	3.63	0.82	8.95	49	3.4 × 10 <sup>-5</sup> (S,B)	ITO/ZnO/BHJ/MoO <sub>3</sub> /Ag	1:1.5	3% DIO	75

Table 1 (Contd.)

Acceptors	LUMO <sup>a</sup> (eV)	HOMO <sup>b</sup> (eV)	Donors	PCE <sup>c</sup> (%)	V <sub>oc</sub> (V)	J <sub>sc</sub> (mA cm <sup>-2</sup> )	FF (%)	μ <sub>e</sub> <sup>d</sup> (cm <sup>2</sup> V <sup>-1</sup> s <sup>-1</sup> )	Device architecture	D/A	Additive	Ref.
3.3b	-3.83(C)	-5.94(C)	PTB7-Th	5.05	0.84	10.60	57	6.0 × 10 <sup>-6</sup> (S,B)	ITO/ZnO/BHJ/MoO <sub>3</sub> /Ag	1 : 1.2	3% DIO	75
3.4a	-3.57(C)	-5.82(C)	PfBT4T-2DT	4.1	0.91	8.0	56	8.3 × 10 <sup>-5</sup> (S,B)	ITO/ZnO/BHJ/V <sub>2</sub> O <sub>5</sub> /Al	1 : 1.4	No additive	78
3.4b	-3.54(C)	-5.64(C)	PfBT4T-2DT	3.1	0.89	6.8	51	8.7 × 10 <sup>-5</sup> (S,B)	ITO/ZnO/BHJ/V <sub>2</sub> O <sub>5</sub> /Al	1 : 1.4	No additive	78
3.5	-3.84(C)	-5.61(C)	PBDT-T-C-T	4.01	0.79	10.6	47.93	4.7 × 10 <sup>-3</sup> (S,B)	ITO/PEDOT:PSS/BHJ/Ca/Al	1 : 1	No additive	79
3.6a	-3.84(C)	-5.48(C)	P3HT	1.95	0.68	5.83	49	3.4 × 10 <sup>-4</sup> (S,B)	ITO/PEDOT:PSS/BHJ/Ca/Al	1 : 2.2	No additive	80
3.6b	-3.76(C)	-5.64(C)	PTB7-Th	3.53	0.81	9.8	44	1.04 × 10 <sup>-5</sup> (S,B)	ITO/ZnO/BHJ/MoO <sub>3</sub> /Al	1 : 1.5	5% CN	81
3.7a	-4.07(C)	-6.22(C)	PBDT-FTTE	2.19	0.91	5.5	41.3	1.7 × 10 <sup>-5</sup> (S,B)	ITO/ZnO/BHJ/MoO <sub>3</sub> /Ag	1 : 2.25	No additive	40
3.7b	-3.74(C)	-5.81(L)	P3HT	1.27	0.54	4.24	55	1 × 10 <sup>-5</sup> (S,B)	ITO/ZnO/BHJ/MoO <sub>3</sub> /Ag	1 : 1	No additive	82
3.7c	-3.76(C)	-5.86(L)	P3HT	0.9	0.57	2.7	58	6 × 10 <sup>-6</sup> (S,B)	ITO/ZnO/BHJ/MoO <sub>3</sub> /Ag	1 : 1	No additive	82
3.7d	-3.72(C)	-5.81(L)	PBDT-F-TT	3.13	0.93	8.6	39	2 × 10 <sup>-4</sup> (S,N)	ITO/ZnO/BHJ/V <sub>2</sub> O <sub>5</sub> /Al	1 : 1.4	No additive	83
3.7e <sub>1</sub>	-3.71(C)	-5.71(L)	P3HT	2.35	0.61	5.92	65	7.1 × 10 <sup>-5</sup> (S,B)	ITO/ZnO/BHJ/MoO <sub>3</sub> /Ag	1 : 1	No additive	82
3.7e <sub>1</sub>	-3.83(H)	-5.9(C)	PTB7-Th	3.0	0.84	11.4	53	—	ITO/ZnO/BHJ/V <sub>2</sub> O <sub>5</sub> /Al	1 : 1.4	No additive	84
3.7e <sub>1</sub>	-3.83(H)	-5.9(C)	PfBT4T-2DT	6.3	0.98	10.7	57	1.8 × 10 <sup>-4</sup> (S,B)	ITO/ZnO/BHJ/V <sub>2</sub> O <sub>5</sub> /Al	1 : 1.4	No additive	84
3.7e <sub>1</sub>	-3.62(C)	-5.99(C)	P3TEA	9.5	1.11	13.27	64.3	—	ITO/ZnO/BHJ/V <sub>2</sub> O <sub>5</sub> /Al	1 : 1.5	2.5% ODT	19
3.7e <sub>1</sub>	-3.62(C)	-5.99(C)	PfBT4T-2DT	6.1	0.965	11.04	57.5	—	ITO/ZnO/BHJ/V <sub>2</sub> O <sub>5</sub> /Al	1 : 1.5	2.5% ODT	19
3.7e <sub>2</sub>	-3.88(C)	-5.83(L)	PTB7-Th	1.72	0.90	4.77	38.6	6.27 × 10 <sup>-5</sup> (S,B)	ITO/ZnO/BHJ/MoO <sub>3</sub> /Ag	1 : 1.5	2.5% CN	85
3.7e <sub>2</sub>	-3.88(C)	-5.83(L)	PfBT4T-2OD	3.05	0.91	5.86	55.4	2.2 × 10 <sup>-5</sup> (S,B)	ITO/ZnO/BHJ/MoO <sub>3</sub> /Ag	1 : 1.5	2.5% CN	85
3.7f	-3.71(C)	-5.71(L)	P3HT	2.28	0.61	6.27	60	1.6 × 10 <sup>-4</sup> (S,B)	ITO/ZnO/BHJ/MoO <sub>3</sub> /Ag	1 : 1	No additive	82
3.8	-3.85(C)	-5.53(C)	BDT-2DPP	3.12	0.95	7.75	42.4	2.3 × 10 <sup>-6</sup> (S,B)	ITO/PEDOT:PSS/BHJ/Ca/Al	1 : 1	No additive	86
3.9	-3.85(C)	-5.92(C)	PPDT2FBT	2.14	0.89	6.04	39.84	1.15 × 10 <sup>-6</sup> (S,B)	ITO/ZnO/BHJ/MoO <sub>3</sub> /Ag	1 : 2	—	87
3.10	-3.72(C)	-5.58(C)	PBDT-T-C-T	0.69	0.84	2.68	30.8	5.02 × 10 <sup>-5</sup> (S,B)	ITO/PEDOT:PSS/BHJ/Ca/Al	1 : 1	No additive	90
4.1a	-3.70(C)	-5.40(C)	PBDT-T-C-T	3.32	0.88	11.92	33.6	2.32 × 10 <sup>-5</sup> (S,N)	ITO/PEDOT:PSS/BHJ/Ca/Al	1 : 1	5% DIO	91
4.1b	-3.8(C)	-5.6(C)	PBDT-T-C-T	1.92	0.90	5.36	39	5.2 × 10 <sup>-6</sup> (S,B)	ITO/PEDOT:PSS/BHJ/Ca/Al	1.25 : 1	3% DIO	94
4.2	-3.86(C)	-6.0(C)	PTB7-Th	5.65	0.83	13.12	52	4.2 × 10 <sup>-5</sup> (S,B)	ITO/ZnO/BHJ/MoO <sub>3</sub> /Ag	1 : 1.5	3% CN	95
4.3	-3.72(C)	-5.77(L)	PBDT-F-TT	5.53	0.91	11.7	52	1 × 10 <sup>-3</sup> (S,N)	ITO/ZnO/BHJ/V <sub>2</sub> O <sub>5</sub> /Al	1 : 1.4	No additive	83
4.3	-3.72(C)	-5.77(L)	PfBT-T3(1,2)-2	6.0	1.029	10.6	54	1.0 × 10 <sup>-3</sup> (S,N)	ITO/ZnO/BHJ/MoO <sub>3</sub> /Al	1 : 1.5	No additive	99
4.4	-3.78(C)	-5.97(C)	PV4T2FBT	5.98	0.90	12.02	54.2	1.93 × 10 <sup>-5</sup> (S,B)	ITO/ZnO/BHJ/V <sub>2</sub> O <sub>5</sub> /Ag	1 : 0.8	2% DIO	96
4.4b	-4.11(C)	-6.24(C)	PTB7-Th	5.34	0.85	13.08	48	1.33 × 10 <sup>-4</sup> (S,B)	ITO/ZnO/BHJ/MoO <sub>3</sub> /Al	1 : 1	1% CN	88
4.4c	-3.88(C)	-5.83(L)	PTB7-Th	5.01	0.87	12	46	2.58 × 10 <sup>-4</sup> (S,B)	ITO/ZnO/BHJ/MoO <sub>3</sub> /Ag	1 : 1.5	2.5% CN	85
4.4c	-3.88(C)	-5.83(L)	PfBT4T-2OD	4.09	0.94	8.21	50.7	8.95 × 10 <sup>-5</sup> (S,B)	ITO/ZnO/BHJ/MoO <sub>3</sub> /Ag	1 : 1.5	2.5% CN	85
4.5a	-3.74(C)	-5.9(L)	PfBT4T-TS1	3.62	0.943	9.65	39.79	1 × 10 <sup>-6</sup> (S,B)	ITO/ZnO/BHJ/MoO <sub>3</sub> /Al	1 : 1.5	3% DPE	142
4.5b	-3.75(C)	-6.0(L)	PfBT4T-2DT	4.3	0.96	9.2	49	2.8 × 10 <sup>-4</sup> (S,N)	ITO/ZnO/BHJ/V <sub>2</sub> O <sub>5</sub> /Al	1 : 1.5	No additive	98
4.5b	-3.75(C)	-6.0(L)	PfBT-T3(1,2)-2	4.7	1.039	8.7	51	2.8 × 10 <sup>-4</sup> (S,N)	ITO/ZnO/BHJ/MoO <sub>3</sub> /Al	1 : 1.5	No additive	99
4.5c	-3.75(C)	-6.0(L)	PfBT4T-2DT	4.2	0.94	8.5	53	3.9 × 10 <sup>-4</sup> (S,N)	ITO/ZnO/BHJ/V <sub>2</sub> O <sub>5</sub> /Al	1 : 1.5	No additive	98
4.5d	-4.0(C)	-5.97(C)	PBDT-F-TT	3.54	0.86	8.39	49	—	ITO/ZnO/BHJ/MoO <sub>3</sub> /Ag	1 : 1.2	3% CN	97
4.5e	-3.68(C)	-5.94(L)	PfBT4T-2DT	1.6	0.92	5.0	37	3.3 × 10 <sup>-5</sup> (S,N)	ITO/ZnO/BHJ/V <sub>2</sub> O <sub>5</sub> /Al	1 : 1.5	No additive	98
4.6	-3.76(C)	-5.86(L)	PfBT-T3(1,2)-2	7.1	0.987	12.5	56	2.3 × 10 <sup>-3</sup> (S,N)	ITO/ZnO/BHJ/MoO <sub>3</sub> /Al	1 : 1.5	No additive	99
4.7	-3.7(C)	-5.8(L)	PTB7-Th	3.64	0.82	9.35	45.55	—	ITO/ZnO/BHJ/MoO <sub>3</sub> /Ag	1 : 1.5	3% CN	101
5.1a	-3.82(C)	-5.87(C)	p-DTS(FBTTh <sub>2</sub> ) <sub>2</sub>	5.13	0.8	10.07	63.6	4.5 × 10 <sup>-4</sup> (S,B)	ITO/PEDOT:PSS/BHJ/Ca/Al	1.3 : 1	0.4% DIO	107
5.1a	—	—	PTB7	3.55	0.84	7.57	55.9	6.85 × 10 <sup>-5</sup> (S,B)	ITO/ZnO/BHJ/MoO <sub>3</sub> /Al	3 : 7	0.4% DIO	110
5.1a	—	—	F-DTS	3.21	0.75	8.09	53	—	ITO/PEDOT:PSS/BHJ/PDIN/Ag	1 : 1	0.4% DIO	111
5.1b	—	—	F-DTS	1.98	0.75	5.88	45	—	ITO/PEDOT:PSS/BHJ/PDIN/Ag	1 : 1	0.4% DIO	111
5.1c	—	—	F-DTS	0.19	0.32	1.52	38	—	ITO/PEDOT:PSS/BHJ/PDIN/Ag	1 : 1	0.4% DIO	111
5.1c	—	—	P3HT	0.01	0.25	0.21	22	—	ITO/PEDOT:PSS/BHJ/Al	1 : 1	No additive	104
5.1d	—	—	F-DTS	—	0	0.42	—	—	ITO/PEDOT:PSS/BHJ/PDIN/Ag	1 : 1	0.4% DIO	111

Table 1 (Contd.)

Acceptors	LUMO <sup>a</sup> (eV)	HOMO <sup>b</sup> (eV)	Donors	PCE <sup>c</sup> (%)	V <sub>oc</sub> (V)	J <sub>sc</sub> (mA cm <sup>-2</sup> )	FF (%)	μ <sub>e</sub> <sup>d</sup> (cm <sup>2</sup> V <sup>-1</sup> s <sup>-1</sup> )	Device architecture	D/A	Additive	Ref.
5.2a	-4.1(-)	-5.9(-)	PBDT-TT-CT	2.78	0.76	9.5	46	8 × 10 <sup>-3</sup> (O <sub>n</sub> N)	ITO/ZnO/BHJ/MoO <sub>3</sub> /Ag	1 : 1	No additive	113
5.2b	-3.86	-5.9	PBDT-S1	5.58	0.80	12.85	53	1.2 × 10 <sup>-3</sup> (S,B)	ITO/PEDOT:PSS/BHJ/Ca/Al	1 : 1	—	51
5.2b	-3.76(C)	-5.87(C)	PTB7-Th	6.41	0.79	13.12	60	4.3 × 10 <sup>-4</sup> (S,B)	ITO/ZnO/BHJ/MoO <sub>3</sub> /Ag	1 : 1	1% DIO & 2% CN	53
5.3	-3.93(C)	-6.01(C)	PBDT-TS1	7.25	0.732	16.52	60.03	1.4 × 10 <sup>-5</sup> (S,B)	ITO/PFN/PBHJ/MoO <sub>3</sub> /Al	1 : 1	7% DPE	114
5.4a	-3.88(C)	-6.16(C)	PTB7-Th	4.36	0.77	10.47	50.4	7.98 × 10 <sup>-4</sup> (S,B)	ITO/ZnO/BHJ/MoO <sub>3</sub> /Al	1 : 2	No additive	117
5.4b	-3.88(C)	-6.16(C)	PTB7-Th	4.42	0.79	10.63	51.47	8.04 × 10 <sup>-4</sup> (S,B)	ITO/ZnO/BHJ/MoO <sub>3</sub> /Al	1 : 2	No additive	117
5.4c	-3.88(C)	-6.16(C)	PTB7-Th	4.68	0.8	10.96	53.3	8.38 × 10 <sup>-4</sup> (S,B)	ITO/ZnO/BHJ/MoO <sub>3</sub> /Al	1 : 2	No additive	117
5.5	-3.98(C)	-6.16(C)	PPDT2FBT	5.28	0.87	10.04	60.16	1.39 × 10 <sup>-5</sup> (S,B)	ITO/ZnO/BHJ/MoO <sub>3</sub> /Ag	1 : 2	No additive	117
5.6	-3.82(C)	-5.96(L)	PBDT-TT-C-T	2.73	0.77	7.83	45	1.78 × 10 <sup>-6</sup> (S,B)	ITO/ZnO/BHJ/PDDOT:PSS/Ag	1 : 1	—	87
6.1	—	—	P3HT	0.29	0.45	2.05	31	—	ITO/PEDOT:PSS/BHJ/Al	1 : 1	3% DIO	118
6.2	-3.83(C)	-5.9(L)	PBT13T	0.65	1.076	1.51	39.29	1.0 × 10 <sup>-4</sup> (O,B)	ITO/ZnO/BHJ/MoO <sub>3</sub> /Ag	1 : 1	No additive	104
6.3	-3.91(C)	-5.92(L)	PBT13T	1.2	1.016	2.44	48.48	4.2 × 10 <sup>-4</sup> (O,B)	ITO/ZnO/BHJ/MoO <sub>3</sub> /Ag	1 : 1	0.5% DIO	126
6.4a	-4.01(C)	-6.02(L)	PBT13T	3.67	1.024	6.56	54.59	2.4 × 10 <sup>-3</sup> (O,B)	ITO/ZnO/BHJ/MoO <sub>3</sub> /Ag	1 : 1	0.5% DIO	126
6.4b	—	—	PBDT-TT-FTTE	3.62	0.81	9.15	48.4	—	ITO/ZnO/BHJ/MoO <sub>3</sub> /Ag	1 : 2.25	0.5% DIO	127
6.5	-3.78(C)	-5.6(C)	PTB7-Th	4.92	0.81	12.74	46	1.79 × 10 <sup>-5</sup> (S,B)	ITO/ZnO/BHJ/MoO <sub>3</sub> /Al	1 : 1.5	5% CN	81
6.6	-3.76(C)	-5.64(L)	PTB7-Th	3.53	0.81	9.8	44	1.04 × 10 <sup>-5</sup> (S,B)	ITO/ZnO/BHJ/MoO <sub>3</sub> /Al	1 : 1.5	5% CN	81
6.7	-3.89(C)	-5.71(C)	PTB7-Th	8.47	0.79	17.9	58	6.1 × 10 <sup>-6</sup> (S,B)	ITO/ZnO/BHJ/MoO <sub>3</sub> /Ag	1 : 1	8% DPE	130
7.2a	-3.77(C)	-6.04(C)	PBDT-TT	6.05	0.803	13.3	56.6	3.4 × 10 <sup>-4</sup> (S,B)	ITO/ZnO/BHJ/MoO <sub>3</sub> /Al	3 : 7	1% DIO & 1% CN	135
7.2b	-3.86(C)	-6.23(C)	PTB7-Th	7.9	0.81	14.5	67	1.5 × 10 <sup>-4</sup> (S,B)	ITO/ZnO/BHJ/MoO <sub>3</sub> /Al	1 : 1.5	1% DIO	136
7.2c	-3.91(C)	-6.26(C)	PTB7-Th	8.3	0.8	15.2	68	1.5 × 10 <sup>-5</sup> (S,B)	ITO/ZnO/BHJ/MoO <sub>3</sub> /Al	1 : 1	1% DIO	136
7.3	-4.04(C)	-6.18(C)	PBDT-TT-FTTE	0.23	0.89	1.51	29.3	3.2 × 10 <sup>-5</sup> (S,B)	ITO/ZnO/BHJ/MoO <sub>3</sub> /Ag	1 : 2.25	1% DIO	40
7.4	-4.03(C)	-6.36(C)	PBDT-TT-FTTE	3.89	0.93	7.68	54.3	4.6 × 10 <sup>-5</sup> (S,B)	ITO/ZnO/BHJ/MoO <sub>3</sub> /Ag	1 : 2.25	1% DIO	40
7.5a	-3.8(C)	-6.01(C)	PTB7-Th	3.29	0.92	8.71	40	3.17 × 10 <sup>-7</sup> (S,B)	ITO/ZnO/BHJ/MoO <sub>3</sub> /Ag	1 : 2	No additive	41
7.5b	-3.77(C)	-5.98(C)	PTB7-Th	6.72	0.94	12.48	58	1.63 × 10 <sup>-4</sup> (S,B)	ITO/ZnO/BHJ/MoO <sub>3</sub> /Ag	1 : 2	2% CN	41
7.5c	-3.76(C)	-5.96(C)	PTB7-Th	5.77	0.92	11.19	55	1.21 × 10 <sup>-4</sup> (S,B)	ITO/ZnO/BHJ/MoO <sub>3</sub> /Ag	1 : 2	2% CN	41
7.6	-3.62(C)	-5.68(L)	PBDT-TT-FTT	4.7	0.94	9.74	49.6	2.27 × 10 <sup>-5</sup> (S,B)	ITO/ZnO/BHJ/MoO <sub>3</sub> /Ag	1 : 3	1% CN	137
7.7a	-3.85(C)	—	PBDT-TT	7.16	0.9	11.98	66.1	2.8 × 10 <sup>-3</sup> (S,B)	ITO/PEDOT:PSS/BHJ/Ca/Al	1 : 1	0.75% DIO	138
7.7a	-3.92(C)	—	PBDT-S-Sc	8.22	0.91	12.9	70	3.5 × 10 <sup>-3</sup> (S,B)	ITO/PEDOT:PSS/BHJ/Ca/Al	1 : 1	0.5% DIO	139
7.7b	-3.87(C)	-6.09(C)	PBDT-TT	8.47	0.91	12.75	73.1	4.8 × 10 <sup>-3</sup> (S,B)	ITO/PEDOT:PSS/BHJ/Ca/Al	1 : 1	0.25% DIO	140
7.8	-3.83(C)	-6.02(L)	PBDT-TT	8.28	1.0	12.32	63.9	1.0 × 10 <sup>-3</sup> (S,B)	ITO/PEDOT:PSS/BHJ/Ca/Al	1 : 1	0.25% DIO	141
7.9	-3.80(C)	-5.97(L)	PBDT-TT	9.28	1.0	12.99	71.5	2.2 × 10 <sup>-3</sup> (S,B)	ITO/PEDOT:PSS/BHJ/Ca/Al	1 : 1	0.75% DIO	141
7.10	-3.68(C)	-6.02(L)	PBDT-TS1	6.17	0.947	13.02	50	9.6 × 10 <sup>-6</sup> (S,B)	ITO/ZnO/BHJ/MoO <sub>3</sub> /Al	1 : 1.5	3% DPE	142
7.11	-3.75(C)	-5.28(C)	PTB7-Th	7.33	0.99	13.24	56	3.66 × 10 <sup>-4</sup> (S,B)	ITO/ZnO/BHJ/MoO <sub>3</sub> /Ag	1.2 : 1	2% CN	143

<sup>a</sup> C and H: measured by CV or obtained by E<sub>HOMO</sub> - E<sub>g</sub>opt. <sup>b</sup> C and L: measured by CV or obtained from E<sub>LUMO</sub> - E<sub>g</sub>opt. <sup>c</sup> Maximum PCE. <sup>d</sup> O and S: measured by OTFT or space charge limited current (SCLC) method; N and B: in neat or blend film.

proved successful in minimizing PDI aggregation.<sup>34</sup> Introduction of alkyl chains or aromatic substituents to the PDI core results in a moderate dihedral angle between the two naphthalene planes and a large dihedral angle between the PDI core and substituent units due to steric effects. Moreover, the substituents also modify PDI with diverse properties, for instance, light absorption, carrier transport, frontier molecular orbitals, miscibility with donor materials and so on.

## 2.1 Mono PDI

X. Zhang *et al.* synthesized a series of solution-processable perylene diimide monomer-based acceptors (molecule 2.1, in Fig. 2) by replacing the 2-methoxyethoxyl groups in molecule 2.1a, one-by-one, with 4,8-bis(5-(2-ethylhexyl)thiophen-2-yl)benzo[1,2-*b*:4,5-*b'*]dithiophene) (BDT) moieties in the bay region.<sup>42</sup> Such structural modification not only enhanced the absorption in the wavelength range from 650 to 800 nm, but also reduced the aggregation tendency as a result of the twisted configuration. Molecule 2.1c (in Fig. 2) was twisted with a dihedral angle of 21° between the two naphthalene planes in the PDI core and 53° between the PDI unit and BDT unit. A smaller domain size of molecule 2.1c around 20 nm was observed while the domain size of its counterpart, molecule 2.1a, was around 0.5–1 μm. Due to the complementary absorption to the donor material, *i.e.* P3HT, and reduced phase size, a higher PCE of 1.66% based on molecule 2.1c was achieved although a sharp decrease of electron mobility comes with a twisted configuration. The electron mobility of P3HT:molecule 2.1a blends was estimated to be  $6.71 \times 10^{-2} \text{ cm}^2 \text{ V}^{-1} \text{ s}^{-1}$ , while it is  $1.96 \times 10^{-5} \text{ cm}^2 \text{ V}^{-1} \text{ s}^{-1}$  for P3HT:molecule 2.1c blends. Yunhao Cai *et al.* reported that when four phenyl groups were attached to the PDI unit at bay positions, molecule 2.2 showed a dihedral angle of 15° between the two naphthalene

planes in the PDI core and 42° between the PDI unit and phenyl unit.<sup>43</sup> With the PTB7-Th:molecule 2.2 blends, a maximum PCE of 4.1% was achieved with a  $V_{oc}$  of 0.87 V, a  $J_{sc}$  of  $10.1 \text{ mA cm}^{-2}$ , and an FF of 46.4%. Since symmetrical bis-substituted PDI derivatives are usually composed of 1,6- and 1,7-isomers,<sup>44</sup> Jinduo Yi *et al.* synthesized a series of mono-aryl-substituted PDI molecules (molecules 2.3a–f, in Fig. 2).<sup>45,46</sup> Results indicated that the *para*-alkyl side chain length showed negligible influence on the spectroscopy and frontier molecular orbital levels of the materials. The propyl substituted compound 2.3a showed the best photovoltaic performance with a PCE of 0.77%,  $V_{oc}$  of 0.63 V,  $J_{sc}$  of  $1.93 \text{ mA cm}^{-2}$ , and FF of 0.63. Then bulky isopropyl groups were introduced on the bay-phenyl unit to finely tune the molecular geometry of mono-substituted PDI derivatives. Although the bulky isopropyl group on the *para*- and *meta*-position of the bay-phenyl group has a negligible influence on optical properties and energy levels, better device performance was achieved using the *meta*-substituted PDI compound 2.3b because of the appropriate nano-scale phase separation and high electron mobility of the blend film.

## 2.2 PDI dimer

Constructing PDI dimers is an effective method to obtain highly efficient NFAs. Two PDI units can be linked by a single bond, single or fused aromatic rings. Molecule 3.1a (in Fig. 3) was linked by a single bond at the bay position which has a torsion angle of 70° between the two PDI units. It has been widely investigated.<sup>47–53</sup> The LUMO and HOMO levels were  $-3.87 \text{ eV}$  and  $-5.95 \text{ eV}$ , respectively. Paired with PBDTTT-C-T, a PCE of 3.63% with a  $V_{oc}$  of 0.73 V, a  $J_{sc}$  of  $10.58 \text{ mA cm}^{-2}$  and an FF of 46.80% was achieved.<sup>47</sup> Since the value of  $V_{oc}$  is closely related to the difference between the HOMO levels of donors and the LUMO levels of acceptors, deeper HOMO levels of donors yield higher  $V_{oc}$ , which provides a higher PCE.<sup>10,54,55</sup> When PBDTTT-CT was replaced by PBDBDD which has deeper HOMO levels, it showed an enhanced  $V_{oc}$  of 0.87 V and FF of 61.1%. Thereby, the PCE was improved to 4.39%.<sup>48</sup> Long Ye *et al.* investigated the selection of donor polymers in achieving high efficiency by combining molecule 3.1a with different donor materials (PBDTPD, PBDTTT-EFT, PSBTBT and PDPP3T, in Fig. 8), which have different energy levels, hole mobility and crystallinity.<sup>50</sup> A PCE of 4.5% was achieved based on PBDTTT-EFT:molecule 3.1a as a result of complementary absorption, well-matched energy levels and moderate crystallinity of PBDTTT-EFT. Due to the high crystallinity, devices based on PDPP3T:molecule 3.1a exhibited a low PCE of 0.98%. Yue Zang *et al.* improved the efficiency of OSCs based on molecule 3.1a further to 5.90% in inverted cell architecture with a PC<sub>61</sub>BM-SAM modified ZnO layer.<sup>49</sup> The  $V_{oc}$ ,  $J_{sc}$  and FF values were 0.8 V,  $11.98 \text{ mA cm}^{-2}$  and 59%, respectively. In their work, a more intense absorption fraction in the inverted device than that in the conventional device was observed. It might be attributed to the different sequences and optical properties of each layer. The inverted devices exhibit higher charge generation than the conventional ones due to better optical distribution. Moreover, in an inverted structure, the metal oxides can provide sufficient

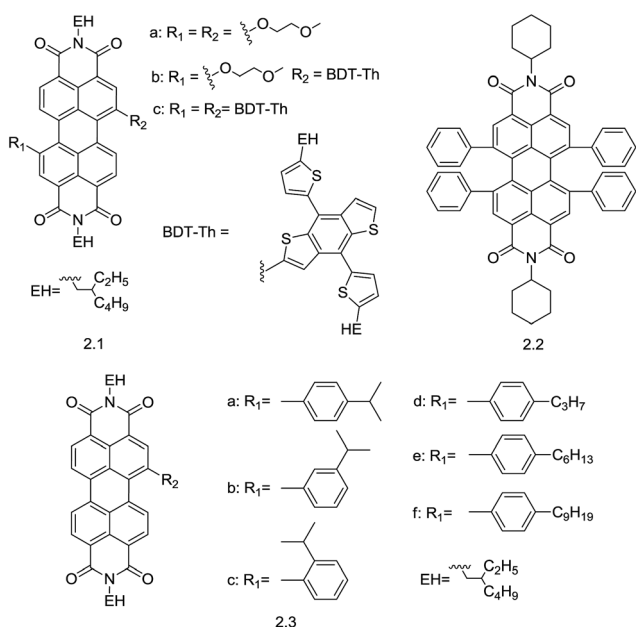


Fig. 2 PDI monomer acceptors substituted *via* bay positions.

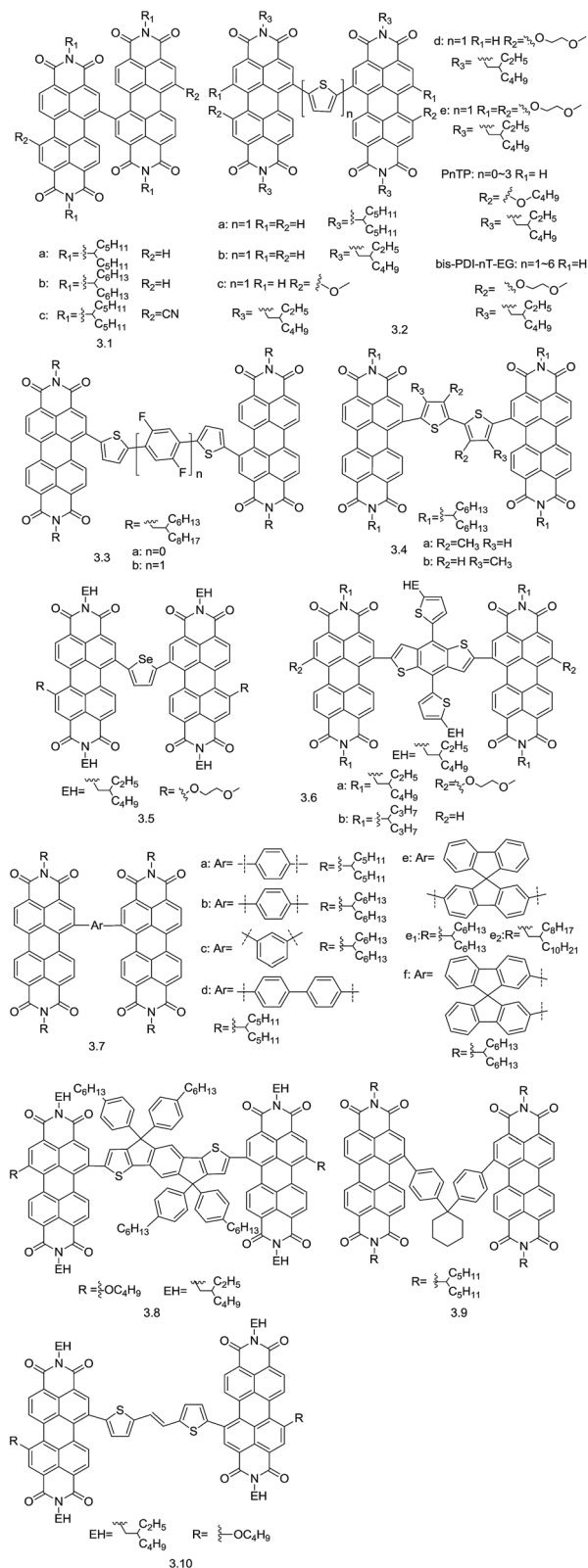


Fig. 3 PDI dimers bridged *via* bay positions.

protection to the active organic layer.<sup>56</sup> It was also reported that the number of donors and acceptors at the active layer surface ( $R_{D/A}$ ) is always larger at the top surface than at the bottom

surface, which is beneficial for charge extraction in the inverted devices.<sup>57</sup> The PC<sub>61</sub>BM-SAM layer was used to passivate the charge-trapping hydroxyl groups on the ZnO layer and help the charge extraction from the BHJ to the electrode, resulting in reduced recombination both in the BHJ layer and BHJ/electrode interface. When strong electron withdrawing cyano groups were attached to molecule **3.1a**, the resulting molecule **3.1c** (in Fig. 3) exhibits a deep LUMO level of  $-4.56$  eV which is the lowest among electron acceptors based on PDI derivatives at present.<sup>58</sup> OSCs based on molecule **3.1c** exhibited a low PCE of 1.4% due to enhanced energy loss which is usually linked to the large LUMO offset between donors and acceptors.<sup>59</sup>

Other than the single bond, the linkage units can also be  $\pi$ -bridges, for example thiophene units.<sup>57,60–68</sup> Xin Zhang *et al.* linked two PDI units *via* a thiophene group, and a PCE of 4.03% was achieved based on molecule **3.2d** (in Fig. 3) with a  $V_{oc}$  of 0.85 V, a  $J_{sc}$  of  $8.86$  mA cm<sup>-2</sup> and an FF of 54.1%.<sup>60</sup> The LUMO and HOMO levels were estimated to be  $-3.84$  eV and  $-5.65$  eV by cyclic voltammetry (CV), which has balanced energy offsets to the polymer donor, PBDTTT-C-T, *i.e.*,  $\Delta E_{LUMO} \approx \Delta E_{HOMO}$  (0.59 eV vs. 0.54 eV). The balanced offsets ensure effective hole and electron transfer in both donor and acceptor phases. It was indicated by molecular modeling that the molecule **3.2d** had a highly twisted configuration with the dihedral angles of  $50$ – $65^\circ$  between the PDI unit and thiophene unit. Compared to its monomeric counterpart molecule **2.1a**, the domain size of which was around several hundred nanometers, molecule **3.2d** showed dramatic reduced aggregation with a phase domain around 30 nm. Besides, molecule **3.2d** showed a broader absorption spectrum owing to intramolecular charge transfer (ICT) transition and extension of the conjugated length. When Xin Zhang *et al.* fine-tuned the parameters of fabrication such as solvent vapor annealing (SVA),<sup>69</sup> annealing time and content of solvent additives used in the film forming process, the mono-molecular and bimolecular recombination reduced and the electron mobility improved.<sup>64</sup> The  $J_{sc}$  significantly increased from  $5.4$  to  $12.85$  mA cm<sup>-2</sup> and a maximum PCE of 6.08% was achieved. By screening the content of additives, the phase separation, phase size and aggregate order can be optimized. It was reported that blends processed with DIO exhibited higher charge mobility as a result of increased structural order as well as phase separation.<sup>61,70</sup> Besides, solvent additives are beneficial for electronic coupling of adjacent PDI aggregates and thus achieve more balanced hole/electron transport.<sup>71,72</sup> It was also reported that surface D/A composition of the active layer can be optimized by adjusting the content of DIO, which can be ascribed to the different boiling points of DIO and the main processing solvent, different solubilities of the donor and acceptor in DIO, and different wettabilities of the donor-DIO and acceptor-DIO solutions on the PEDOT:PSS or ZnO substrates.<sup>57,64,68</sup> In the work of Zhenhuan Lu and co-workers in the active layer of PBDTT-C-T:molecule **3.2c**, as [DIO] ranges from 0 to 15%, the  $R_{D/A}$  on the top surface was in the range of 2.0–5.3 while the  $R_{D/A}$  on the bottom surface was in the range of 0.3–0.84.<sup>57</sup>  $R_{D/A}$  on both the top and bottom surfaces showed an increasing tendency with the content of DIO increasing. The best PCE of 4.34% in the inverted devices was obtained at a low

[DIO] of 2%, while the best PCE of 3.28% in conventional devices was obtained at a high [DIO] of 7% (as shown in Table 1). The holes are extracted from the bottom surface in the conventional devices and the electrons are extracted from the bottom surface in the inverted ones. At low [DIO], the bottom surface exhibited low  $R_{D/A}$ , *i.e.* acceptor abundance, which was favourable for electron extraction in the inverted devices. At higher [DIO], relatively higher donor abundance was favourable for hole extraction in the conventional devices. In addition, whether in the inverted devices or conventional devices, devices processed without [DIO] exhibited the lowest PCE. Recently, Xin Zhang *et al.* improved the PCE of molecule **3.2d** based OSCs further to 7.24% by integration of film-morphology optimization, and cathode interlayer engineering and using PBDT-TS1 as the donor material.<sup>65</sup> A combination of solvent annealing (SA) and SVA treatments was used to optimize film morphology, which helped to achieve more balanced hole/electron mobility. Additionally, Ca and PDINO were used as the cathode layer in their work to reduce bimolecular loss. Zhenhuan Lu *et al.* synthesized molecule **3.2b**, molecule **3.2d** and molecule **3.2e** (in Fig. 3) to investigate the impact of molecular solvophobicity *versus* solvophilicity on the performance of devices based on PDI.<sup>73</sup> 2-Methoxyethoxyl (EG) groups were introduced to the thiophene-bridged PDI dimers at bay positions to adjust molecular solvophobicity (0 EG for molecule **3.2b**, 2 EG for molecule **3.2d** and 4 EG for molecule **3.2e**). With the number of EG groups increasing, molecular solvophobicity *versus* solvophilicity and solution-processability improved, and the strong aggregation ability reduced. In consequence, the best PCE of OSC devices improved from 0.41% for molecule **3.2b** to 0.76% for molecule **3.2d** and then further to 1.54% for molecule **3.2e** when using P3HT as the donor material. Jiayu Wang *et al.* synthesized a set of bay-linked PDI dimers with different oligothiophene bridges, namely molecules **P0TP-P3TP** (in Fig. 3) used as electron acceptors in BHJ OSCs.<sup>63</sup> The length of spacers had a great influence on the absorption properties, energy levels, electron mobility, morphology and so on. With the introduction of the thiophene unit, the dihedral angles between two PDI units reduced, and the miscibility with the polymer donor increased, resulting in smoother morphology in blend films. With increasing length of oligothiophene bridges, the absorption spectra red shifted and the maximum extinction coefficients increased. However, the electron mobility decreased from  $2.4 \times 10^{-4}$  to  $4 \times 10^{-5} \text{ cm}^2 \text{ V}^{-1} \text{ s}^{-1}$  in the active layer blended with PBDTTT-C-T with increasing length of oligothiophene bridges ( $n = 1-3$ ). Molecule **P0TP** ( $n = 0$ ) exhibited the lowest electron mobility of  $7 \times 10^{-6} \text{ cm}^2 \text{ V}^{-1} \text{ s}^{-1}$ . Molecule **P1TP** with one thiophene unit as the spacer has the highest electron mobility and the best PCE. The spacer geometry also has a great influence on the performance of acceptors based on PDI dimers. In the work of Xin Zhang and co-workers, they increased the number of thiophene units to six and synthesized molecules **bis-PDI-1T-EG** to **bis-PDI-6T-EG** (in Fig. 3).<sup>74</sup> As the length of the oligothiophene bridge increased, the absorption in the near IR region from 650 to 900 nm increased due to ICT absorption from oligothiophene units to PDI units. The HOMO levels increased from  $-5.65$  to  $-5.10$  eV, while there was little

change in LUMO levels. It was reported that the HOMO levels were mainly related to oligothiophene units, while the LUMO levels were mainly determined by perylene in these molecules. Wisnu Tanyo Hadmojo and co-workers reported two PDI dimers, molecule **3.3a** and molecule **3.3b** (in Fig. 3).<sup>75</sup> Molecule **3.3a** was bridged by a bithiophene unit and molecule **3.3b** was obtained by inserting a 2,5-difluorobenzene (F2B) moiety to the spacer. Due to noncovalent S-F coulombic interaction,<sup>76,77</sup> the planarity of the spacer in molecule **3.3b** was improved compared to that in molecule **3.3a**. Molecule **3.3b** showed a dihedral angle of  $2.7^\circ$  between the F2B unit and the thiophenes while the dihedral angle between two thiophene units in molecule **3.3a** was  $21.5^\circ$ . Thereby molecule **3.3b** exhibited enhanced intermolecular packing which resulted in higher electron mobility ( $3.4 \times 10^{-5} \text{ cm}^2 \text{ V}^{-1} \text{ s}^{-1}$  vs.  $6.0 \times 10^{-6} \text{ cm}^2 \text{ V}^{-1} \text{ s}^{-1}$ ). In addition, molecule **3.3b** still showed a twisted configuration with a dihedral angle of  $59.6^\circ$  between the spacer and PDI moieties which prevented excessive phase aggregation. In consequence, a higher PCE of 5.05% was achieved based on molecule **3.3b** with a  $V_{oc}$  of 0.84 V, a  $J_{sc}$  of  $10.60 \text{ mA cm}^{-2}$ , and an FF of 57% while a PCE of 3.63% was achieved based on molecule **3.3a** with a  $V_{oc}$  of 0.82 V, a  $J_{sc}$  of  $8.95 \text{ mA cm}^{-2}$ , and an FF of 49%. Jingbo Zhao *et al.* studied the relationship between the spacer geometry and the OSC performances by designing molecule **3.4a** and molecule **3.4b** in which two PDI moieties were linked by bithiophene spacers with two methyl groups attached to different locations as shown in Fig. 3.<sup>78</sup> The small difference in the chemical structures of molecules **3.4a** and **3.4b** resulted in significant difference in molecular geometry. The dihedral angles between the two PDI moieties are about  $60^\circ$  in molecule **3.4a** and  $90^\circ$  in molecule **3.4b**, and the dihedral angles between the two thiophene rings were  $54^\circ$  and  $17^\circ$  in molecules **3.4a** and **3.4b**, respectively, resulting in a smaller domain size of molecule **3.4a** than that of molecule **3.4b** in the blend films when they were paired with PffBT4T-2DT (in Fig. 8). In consequence, a PCE of 4.1% was achieved based on molecule **3.4a** with a  $V_{oc}$  of 0.91 V, a  $J_{sc}$  of  $8.0 \text{ mA cm}^{-2}$ , and an FF of 56% while a PCE of 3.1% was achieved based on molecule **3.4b** with a  $V_{oc}$  of 0.89 V, a  $J_{sc}$  of  $6.8 \text{ mA cm}^{-2}$ , and an FF of 51%. Xin Zhang *et al.* reported a new PDI acceptor molecule **3.5** (in Fig. 3) by replacing the thiophene unit in molecule **3.2d** with a selenophene unit.<sup>79</sup> When paired with PBDTTT-C-T without the use of additives, a PCE of 4.01% was achieved based on molecule **3.5** with a  $V_{oc}$  of 0.79 V, a  $J_{sc}$  of  $10.60 \text{ mA cm}^{-2}$ , and an FF of 47.93%. As shown in Fig. 3, other aromatic units were also used to construct the PDI dimer, for instance, BDT (molecule **3.6**),<sup>80,81</sup> phenyl (molecules **3.7a**, **3.7b**, **3.7c**),<sup>40,82</sup> biphenyl (molecule **3.7d**, in Fig. 3),<sup>83</sup> 9,9'-spiro[9H-fluorene] (SBF) (molecules **3.7e**, **3.7f**),<sup>19,82,84,85</sup> indaceno [1,2-*b*:5,6-*b'*] dithiophene (IDT) (molecule **3.8**),<sup>86</sup> 1,1-diphenylcyclohexane (molecule **3.9**),<sup>87</sup> *etc.* Among these PDI dimers, molecule **3.7e** bridged by SBF was the mostly studied dimer. Molecule **3.7e**<sub>1</sub> was first reported by Qifan Yan and co-workers.<sup>82</sup> SBF exhibits an orthogonal molecular structure, where two planar fluorene units are connected through a spiro- $\text{sp}^3$  carbon.<sup>88,89</sup> When molecule **3.7e**<sub>1</sub> was paired with P3HT, a PCE of 2.35% was achieved. When molecule **3.7e**<sub>1</sub> was combined with a well matched donor PffBT4T-2DT, a PCE of 6.3% was achieved with a  $V_{oc}$  of 0.98 V, a  $J_{sc}$  of  $10.7 \text{ mA cm}^{-2}$  and an FF of 57%.<sup>84</sup> Interestingly, the LUMO offset

between PffBT4T-2DT and molecule **3.7e<sub>1</sub>** was merely 0.12 eV. When molecule **3.7e<sub>1</sub>** was combined with P3TEA (in Fig. 8), an impressive PCE of 9.5% was achieved with negligible driving force (energy difference between the bandgap and charge transfer states) in OSC devices.<sup>19</sup> The LUMO levels and HOMO levels were determined to be  $-3.62$  eV and  $-5.99$  eV for molecule **3.7e<sub>1</sub>**, and  $-3.57$  eV and  $-5.37$  eV for P3TEA by CV. Although the LUMO offset was merely 0.05 eV in the P3TEA:molecule **3.7e<sub>1</sub>** combination, there was still efficient charge generation and separation. The OSC devices exhibited a low voltage loss of 0.61 V and an impressive  $V_{oc}$  of 1.11 V. In contrast, a PCE of 6.1% was achieved with a  $V_{oc}$  of 0.965 V, a  $J_{sc}$  of  $11.04$  mA cm<sup>-2</sup> and an FF of 57.5% based on PffBT4T-2DT:molecule **3.7e<sub>1</sub>** which exhibited a driving force of 0.16 eV, and a PCE of 7.0% was achieved with a  $V_{oc}$  of 0.954 V, a  $J_{sc}$  of  $12.46$  mA cm<sup>-2</sup> and an FF of 59.1% based on P3TEA:molecule **3.1b** which exhibited a driving force of 0.2 eV. Their work showed that a small driving force was sufficient for charge separation. S. Dai *et al.* synthesized molecule **3.10** by linking two perylene diimide units by thienylene vinylene.<sup>90</sup> Although it exhibited strong absorption in the visible region (300–800 nm), an OSC based on PBDTTT-C-T:molecule **3.10** exhibited a PCE of 0.69%.

### 2.3 Core(PDI)<sub>n</sub>

One advantage of fullerene derivatives is their ball or near-ball-shape structures which can possibly form a 3D charge-transporting network.<sup>1</sup> PDI derivatives can also potentially possess a quasi-3D nonplanar structure. Usually, with the help of the steric effect, these PDI acceptors with 3D geometry exhibit interlocking or compact molecular structures that PDI moieties orientate to different directions. This suppresses aggregation of acceptors in BHJ blend films efficiently and facilitates nano-scale phase domain formation. Besides, it benefits energy transfer and electron transport among PDI moieties. More importantly, it enables multidimensional charge transport and separation.

Yuze Lin *et al.* reported a star-shaped molecule **4.1a** (in Fig. 4) with a triphenylamine (TPA) core which possesses a quasi-3D nonplanar structure and isotropic optical and charge-transporting properties.<sup>91</sup> TPA exhibited a starburst molecular structure due to the sp<sup>3</sup> hybrid orbital of the core nitrogen atom.<sup>9</sup> It was often used to construct a star-shaped structure.<sup>91–93</sup> Molecule **4.1a** showed weak molecular aggregation and strong absorption in the visible region which was complementary to that of common low bandgap polymer donors. A maximum PCE of 3.45% was achieved based on molecule **4.1a** with a high  $J_{sc}$  of  $11.92$  mA cm<sup>-2</sup> and a moderate  $V_{oc}$  of 0.88 V. However, it showed a low FF of 33.6% which might be attributed to an unbalanced electron/hole mobility ( $7.17 \times 10^{-4}$  cm<sup>2</sup> V<sup>-1</sup> s<sup>-1</sup>/  $2.32 \times 10^{-5}$  cm<sup>2</sup> V<sup>-1</sup> s<sup>-1</sup>). Qichao Wu synthesized an acceptor with perylene diimide linked through a thiophene ring with TPA, *i.e.* molecule **4.1b** (in Fig. 4).<sup>94</sup> A strong absorption peak appeared in the 330 nm to 450 nm region because introduction of the thiophene unit resulted in an extended molecular absorption spectrum. OSCs based on a PBDTTT-C-T:molecule **4.1b** blend film with a 3% DIO additive

exhibited PCE of 1.92%. Shuixing Li and co-workers synthesized a PDI trimer, molecule **4.2** (in Fig. 4), in which three PDI units were attached to one benzene core.<sup>95</sup> It showed a twisted molecular geometry with a compact arrangement of sterically bulky PDI moieties. In the PTB7-Th:molecule **4.2** blends, PDI trimers formed nano-sized molecular particles with the aromatic  $\pi$  surface towards the outside. The short-range stacking of PDI molecules facilitates electron transport. A maximum PCE of 5.65% with a  $V_{oc}$  of 0.83 V, a  $J_{sc}$  of  $13.12$  mA cm<sup>-2</sup>, and an FF of 52% was achieved for the device. A tetraphenylethylene (TPE) core-based molecule **4.3** (in Fig. 4), TPE-PDI<sub>4</sub>, with a unique 3D molecular structure of a four-wing propeller-shape was reported by Yuhang Liu *et al.*<sup>83</sup> Whereas the HOMO, LUMO, and UV-Vis spectrum of molecule **4.3** are similar to those of molecule **3.7d**, TPE-PDI<sub>4</sub> exhibits enhanced electron mobility ( $1 \times 10^{-3}$  cm<sup>2</sup> V<sup>-1</sup> s<sup>-1</sup> vs.  $2 \times 10^{-4}$  cm<sup>2</sup> V<sup>-1</sup> s<sup>-1</sup>) and smaller domain size (20 nm vs. 60–80 nm). It indicates that the 3D structure can facilitate charge transport. Spiro-bifluorene is a rigid perpendicular unit which is favorable for constructing 3D geometry. Jaewon Lee *et al.* reported a 3D PDI acceptor, molecule **4.4** (in Fig. 4) with a spiro-bifluorene core.<sup>96</sup> It exhibited an interlocking geometry which reinforced uniformity of the molecular conformation. A PCE of 5.98% was achieved with a  $V_{oc}$  of 0.9 V, a  $J_{sc}$  of  $12.02$  mA cm<sup>-2</sup> and an FF of 54.2% in devices based on PV4T2FBT:molecule **4.4** blends. Lei Yang and co-workers made a comparison between molecule **4.4c** (in Fig. 4) and molecule **3.7e<sub>2</sub>**.<sup>85</sup> In devices based on both PTB7-Th:acceptor and PffBT4T-2OD:acceptor blends, molecule **4.4c** outperformed molecule **3.7e<sub>2</sub>**. As shown in Table 1, the PCEs were 5.01% vs. 1.72% with PTB7-Th:acceptor blends and 4.09% vs. 3.05% with PffBT4T-2OD:acceptor blends. Besides, molecule **4.4c** exhibited higher electron mobility. It once again indicated that the 3D structure with a compact and interlocked configuration was favourable for achieving high efficiency in OSC devices. Shi-Yong Liu and co-workers reported a 3D PDI acceptor, molecule **4.5c** (in Fig. 4), in which the tetraphenylsilane core was coupled with four PDI units.<sup>97</sup> These four PDI units were compact, interlocked, and non-rotatable. When molecule **4.5c** was combined with PBDTT-F-TT, a PCE of 3.54% was achieved with a  $V_{oc}$  of 0.86 V, a  $J_{sc}$  of  $8.39$  mA cm<sup>-2</sup> and an FF of 49%. Yuhang Liu and co-workers made a comparison among molecule **4.5b**, molecule **4.5d** and molecule **4.5e**, which had different core atoms (in Fig. 4).<sup>98</sup> Although the sizes of the core atoms were different (C < Si < Ge), they showed similar 3D molecular structures and optical bandgaps. All blend films of PffBT4T-2DT with these three molecules exhibited smooth morphology and relatively small domains. However, they performed differently in the OSC devices. A PCE of 4.3% was achieved in devices based on PffBT4T-2DT:molecule **4.5b** with a  $V_{oc}$  of 0.96 V, a  $J_{sc}$  of  $9.2$  mA cm<sup>-2</sup> and an FF of 49% and a PCE of 4.2% was achieved in devices based on PffBT4T-2DT:molecule **4.5d** with a  $V_{oc}$  of 0.94 V, a  $J_{sc}$  of  $8.5$  mA cm<sup>-2</sup> and an FF of 53% while a PCE of 1.6% was achieved in devices based on PffBT4T-2DT:molecule **4.5e** with a  $V_{oc}$  of 0.92 V, a  $J_{sc}$  of  $5.0$  mA cm<sup>-2</sup> and an FF of 37%. As shown in Table 1, the low PCE of molecule **4.5d** could be attributed to the much lower electron mobility. Since excessive extent of twisting would hurt the charge mobility of

the NFA, a comparative study of photovoltaic performance among molecules **4.3**, **4.5b** and **4.6** (in Fig. 4) with different extents of the intramolecular twisting was performed by Haoran Lin *et al.*<sup>99</sup> Compared to molecules **4.3** and **4.5b**, the tetraphenylpyrazine (TPPz) core in molecule **4.6** is less twisted because not only the core is bigger in size but also there are no hydrogen atoms attached to the center pyrazine unit. The electron mobility of pure molecule **4.6** was estimated to be as high as

$(2.3 \pm 0.2) \times 10^{-3} \text{ cm}^2 \text{ V}^{-1} \text{ s}^{-1}$ . The authors ascribed the blue-shift of the main absorption peak of molecule **4.6** from solution to film to the H-aggregation process in the film. Although molecule **4.6** exhibits the lowest extent of intramolecular twisting and thus a stronger aggregation, reasonably small domain size and clear phase separation were observed in the blend film based on PffBT-T3(1,2)-2:molecule **4.6**. The highest PCE of 7.1% was achieved in the inverted devices using molecule **4.6** as the acceptor with a  $V_{oc}$  of 0.99 V, a  $J_{sc}$  of  $12.7 \text{ mA cm}^{-2}$  and an FF of 57%. As the extent of intramolecular twisting increases, the PCEs decrease not only in the blend of PffBT-T3(1,2)-2:molecule **4.6**, but also in the blend of P3HT:molecule **4.6** and PTB7-Th:molecule **4.6**. 9,9'-Bifluorenylidene, which could be used as an electron acceptor in BHJ OSCs,<sup>100</sup> was chosen as the core to construct the (core)PDI<sub>n</sub>-type twisted acceptor, *i.e.* molecule **4.7** (in Fig. 4).<sup>101</sup> Devices incorporating PTB7-Th as the electron donor outperformed those based on PTB7, largely due to higher short-circuit current density ( $J_{sc}$ ), which may be a result of the broadened absorption coverage of the blend of PTB7-Th:molecule **4.7** relative to that of PTB7:molecule **4.7**. Optimized PCE of 3.64% was achieved for PTB7-Th:molecule **4.7** with a  $V_{oc}$  of 0.82 V, a  $J_{sc}$  of  $9.35 \text{ mA cm}^{-2}$  and an FF of 45.55%.

In conclusion, the photoelectric and physical properties of PDI derivatives modified *via* the bay position vary with different substituents. (1) Molecular geometry. Molecular geometry, which can be modified by choosing appropriate spacer units, significantly affects the packing behaviour, electron mobility and film morphology, which has close relationship with the exciton diffusion/separation, charge transport, and, finally, the PCE. (2) Light absorption. Usually, PDI derivatives linked *via* bay positions exhibit strong absorption in the visible region of 400–600 nm, and introducing electron-donating groups can extend the absorption band. (3) Energy levels. Introduction of electron-withdrawing units leads to lower LUMO energy levels while electron-donating units have an inverse effect. Novel acceptors with twisted molecular geometry, high electron mobility, complementary absorption spectrum, appropriate energy levels, which can also form good film morphology with the polymer donor, are quite promising.

### 3. Imide positions

Functionalization at the bay position can form a twisted configuration, providing a good solution to inhibit aggregation. However, it also disturbs the planarity of the PDI core, and weakens the interaction between the molecules. Planarity is believed to favor solid-state packing and carrier transport. Intermolecular electronic orbital overlap within the stacks is essential for electron transport materials. It enhances mobility compared to that in amorphous materials.<sup>102</sup> The crystallinity of the acceptor domains promotes charge delocalization, thereby increasing charge dissociation. Geminate recombination loss of bound polaron pairs can be reduced by ordering the solid state. Functionalization at imide positions is the simplest way to modify PDI without twisting the PDI core, but it is less investigated than functionalization at bay positions due to the

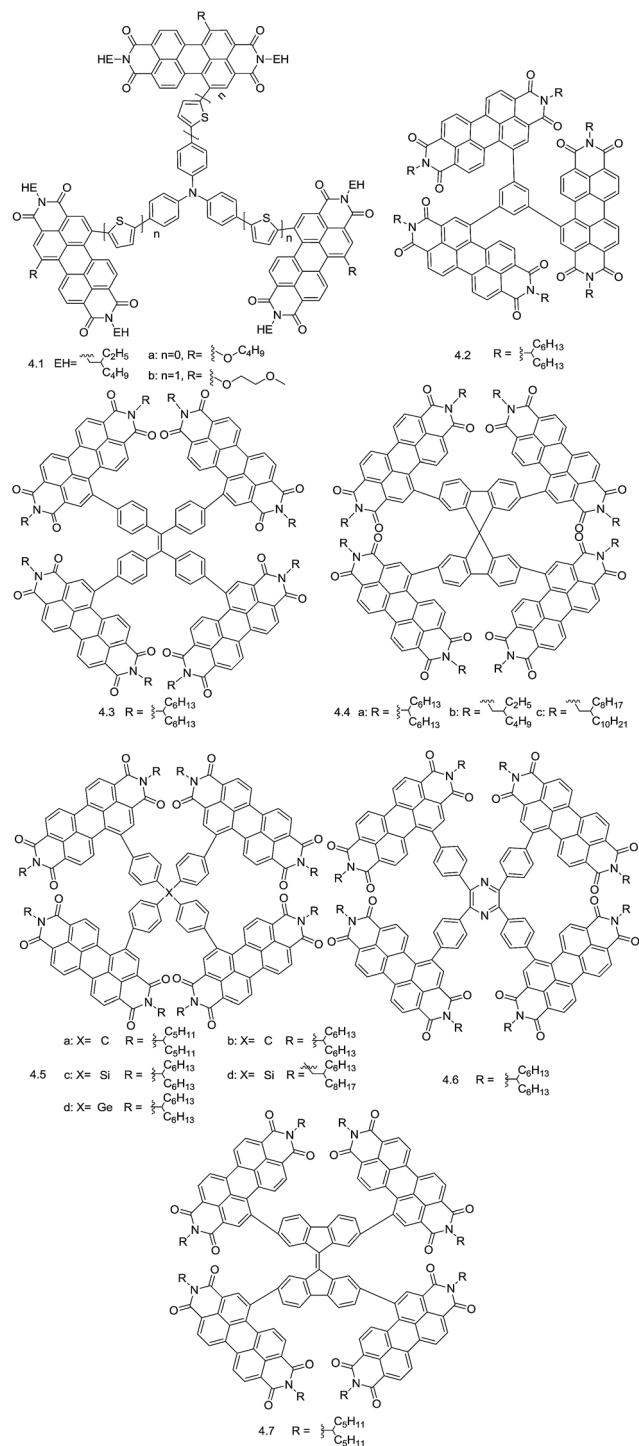


Fig. 4 Multidimensional PDIs substituted *via* bay positions.

limited substituents and little effect on the optical and electronic properties of PDIs.<sup>103</sup>

At first, alkyl chains and aromatic groups were introduced to imide positions of PDI monomers. They notably affect the solubility and molecular packing behaviors of PDI derivatives. Alkyl side chains of “swallow tail” at the imide positions can disturb the packing structure and thus minimize the formation of large PDI domains. PDI with alkyl chains at the nitrogen position can be readily synthesized. Hence, they were widely investigated. They exhibit good solubility, crystallinity, and PCEs ranging from 1% to 5% in different devices.<sup>70,71,104–111</sup> The best PCE of 5.13% was obtained for the device based on *p*-DTS(FBTTh<sub>2</sub>)<sub>2</sub>:molecule **5.1a** (in Fig. 5) with a  $J_{sc}$  of 10.07 mA cm<sup>-2</sup>, a  $V_{oc}$  of 0.80 V, and an FF of 63.6%. Jon-Paul Sun and co-workers studied the impact of alkyl side chains on the photovoltaic performance of PDIs in OSC cells by comparison of molecules **5.1a–5.1d** (in Fig. 5). The alkyl side chains drastically affect the solubility, film formation, and packing behaviors of PDI. When paired with F-DTS, molecule **5.1a** showed the best PCE of 3.21% while molecule **5.1d** showed negligible PCE. Besides, all of the molecules exhibited good solubility, but molecule **5.1d** showed significantly lower solubility. Because the 2-ethylhexyl side chain has a branching point on carbon 2 as opposed to carbon 1, branching at carbon 2 has a lower sterical effect and it exhibited enhanced  $\pi$ - $\pi$  stacking among PDI chromophores.

Heinz Langhals and Wolfgang Jona linked two PDI units with a hydrazine bond at the imide position with different alkyl chains, with yields ranging from 29% to 56%.<sup>112</sup> The PDI dimer, molecule **5.2a** (in Fig. 5), which was demonstrated to be a potential alternative to fullerenes, is highly rigid with a 90° torsion angle between the two PDI planes. It was reported by Sridhar Rajaram and co-workers that the blend films consisting of the polymer donor PBDTTT-C-T and molecule **5.2a** showed broad spectral coverage and moderate phase separation, yielding device efficiency of 2.78% with a  $J_{sc}$  of 9.5 mA cm<sup>-2</sup>, a  $V_{oc}$  of 0.76 V and a FF of 0.46.<sup>113</sup> As is well known, the alkyl chains also affect the device performance.<sup>52</sup> By shortening the alkyl side chain, molecule **5.2b** was obtained. Additionally, by adjusting the polymer donor material, the efficiency can be further improved. In Chen-Hao Wu and co-workers' work, a promising PCE of 6.41% was achieved for the PTB7-Th:molecule **5.2b** BHJ devices with a LUMO offset of 0.12 eV, while the bay-linked counterpart molecule **3.1a** demonstrated a PCE of 5.56%.<sup>53</sup> The  $V_{oc}$ ,  $J_{sc}$ , and FF values of OSCs based on molecule **5.2b** and molecule **3.1a** were 0.79 V vs. 0.79 V, 13.12 mA cm<sup>-2</sup> vs. 12.86 mA cm<sup>-2</sup>, and 60% vs. 54%, respectively. This difference can be ascribed to the charge mobility. Both of them had good miscibility with PTB7-Th, while the rigid molecule **5.2b** also maintained appropriate aggregation domains which were favorable for charge transport. Besides, it was demonstrated by two-dimensional grazing-incidence wide-angle X-ray scattering (2D GIWAXS) that the bay-linked dimer, molecule **3.1a** disrupted the  $\pi$ - $\pi$  stacking of the polymer donor severely, while PTB7-Th:molecule **5.2b** blend film did not. Hence PTB7-Th:molecule **5.2b** blend film exhibited higher charge mobility ( $4.3 \times 10^{-4}$  cm<sup>2</sup> V<sup>-1</sup> s<sup>-1</sup> vs.  $9.4 \times 10^{-5}$  cm<sup>2</sup> V<sup>-1</sup> s<sup>-1</sup> for electron

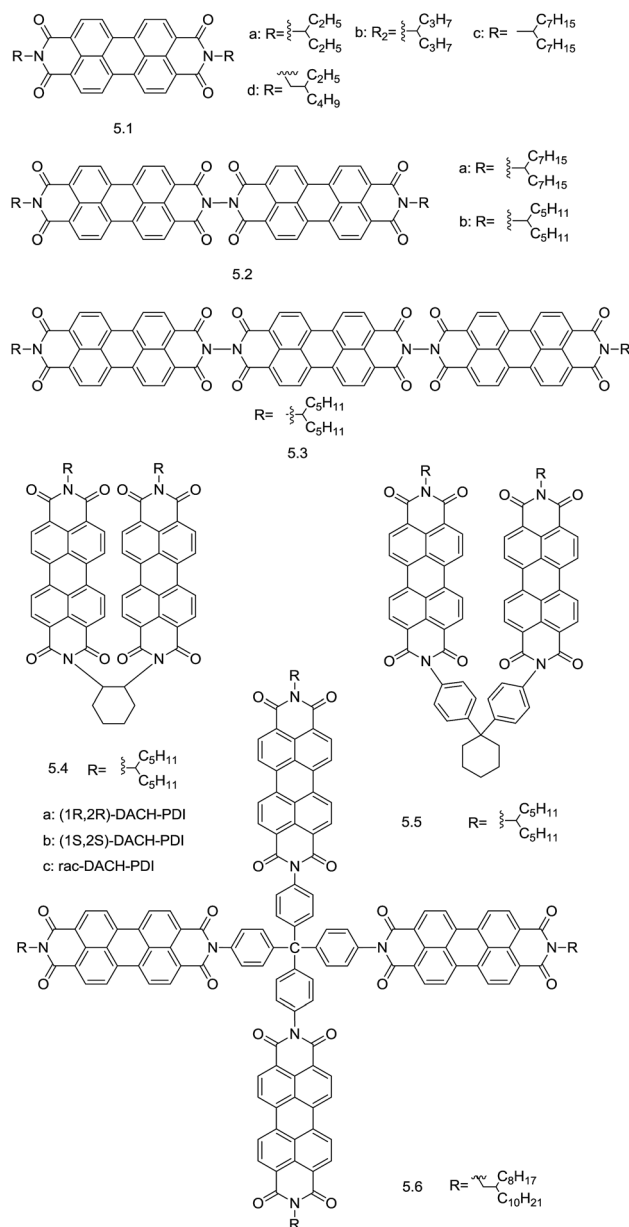


Fig. 5 Acceptors substituted *via* imide positions.

mobility and  $2.3 \times 10^{-2}$  cm<sup>2</sup> V<sup>-1</sup> s<sup>-1</sup> vs.  $1.7 \times 10^{-2}$  cm<sup>2</sup> V<sup>-1</sup> s<sup>-1</sup> for hole mobility). Ningning Liang and co-workers reported a PDI trimer as an acceptor linked *via* the imide position with a synthesis yield of 28%.<sup>114</sup> A PCE as high as 7.25% was achieved based on PBDT-TS1:molecule **5.3** blends. It exhibited a  $V_{oc}$  of 0.732 V, a high  $J_{sc}$  of 16.52 mA cm<sup>-2</sup>, and an FF of 60.03%. It was reported that by increasing the amount of PDI units *via* imide positions in PDI oligomers, the extinction coefficient can be strikingly improved. More importantly, despite the nodes in both the HOMO and LUMO of PDI, linking PDI molecules *via* an N-N bond helps to change their reduction potential.<sup>115</sup> When the PDI moieties are isoenergetic, rapid electron hopping can be found in these linear PDI oligomers.<sup>116</sup> It acts as a complementary charge transfer route to intermolecular interactions based on  $\pi$ - $\pi$  stacking. Attaching multiple PDI units *via* the imide

position provides a potential method of molecule design for acceptors based on PDI derivatives.

The properties of functionalized PDI derivatives at the imide position also varied with the linkage units. For example, Guangpeng Gao and co-workers reported a set of chiral PDI dimers, molecules **5.4a–5.4c** (in Fig. 5) which were bridged with twisted 1,2-diaminocyclohexane (DACH).<sup>117</sup> Devices based on PDI dimers bridged with racemic DACH (molecule **5.4c**) showed a maximum PCE of 4.68%, which is superior to 4.42% of a PDI dimer bridged with enantiomerically pure 1*R*,2*R*-DACH (molecule **5.4a**) and 4.36% of a PDI dimer bridged with 1*S*,2*S*-DACH (molecule **5.4b**). Better miscibility between molecule **5.4c** and the donor polymer might account for the superiority. GiEun Park and co-workers reported a V-shaped PDI dimer which was linked by a  $sp^3$ -bridge, 1,1-diphenylcyclohexane *via* imide positions.<sup>87</sup> Compared to its bay-linked counterpart molecule **3.9** (in Fig. 3), molecule **5.5** (in Fig. 5) exhibited higher electron mobility ( $1.39 \times 10^{-5} \text{ cm}^2 \text{ V}^{-1} \text{ s}^{-1}$  vs.  $1.15 \times 10^{-6} \text{ cm}^2 \text{ V}^{-1} \text{ s}^{-1}$ ) and appropriate multi-dimensional interconnectivity of donor and acceptor phases in the BHJ blend. What's more, PPDT2FBT:molecule **5.5** blends showed relatively balanced charge transport ( $\mu_h/\mu_e \approx 7.70$ ), compared to that in PPDT2FBT:molecule **3.9** blends ( $\mu_h/\mu_e \approx 37.04$ ), which explained the higher FF of PPDT2FBT:molecule **5.5** blends. Hence, a higher PCE of 5.28% was achieved with a  $J_{sc}$  of  $10.04 \text{ mA cm}^{-2}$ , a  $V_{oc}$  of 0.87 V, and an FF of 60.16% in devices based on PPDT2FBT:molecule **5.5** blends, while a PCE of 2.14% was achieved with a  $J_{sc}$  of  $6.04 \text{ mA cm}^{-2}$ , a  $V_{oc}$  of 0.89 V and an FF of 39.84% in devices based on PPDT2FBT:molecule **3.9** blends. Tetraphenyl methane was selected by Wangqiao Chen *et al.* to construct a quasi-3D non-planar structure due to its tetrahedral architecture.<sup>118</sup> Molecule **5.6** (in Fig. 5) possesses a dihedral angle of  $110.17^\circ$  between the PDI units and the phenyl core. A PCE of 2.73% was reported with a  $V_{oc}$  of 0.77 V, a  $J_{sc}$  of  $7.83 \text{ mA cm}^{-2}$ , and an FF of 45.0% based on PBDTTT-C-T:molecule **5.6**.

## 4. *ortho* positions

Since the functionalization at 2,5,8,11-positions of PDI was fulfilled by Satomi Nakazono *et al.* in 2009, it has been widely investigated.<sup>119,120</sup> Usually, functionalization at *ortho* positions is achieved *via* ruthenium catalyzed reactions or iridium catalyzed reactions.<sup>121,122</sup> Substitutions at *ortho* positions maintain the planarity of the perylene  $\pi$ -plane, which provides a promising method to tune the properties of perylene dyes without geometric distortion of the PDI core.<sup>32,123</sup>

Valentin Kamm and co-workers made a comparison between *ortho*-substituted molecule **6.1** (in Fig. 6) and molecule **5.1c** (in Fig. 5) which had similar molecular weights.<sup>104</sup> A higher PCE of 0.29% was achieved in devices based on molecule **6.1** than those based on molecule **5.1c** when using P3HT as the donor material. It was indicated by time-resolved photoluminescence spectroscopy that a H-aggregate formed between chromophores in molecule **5.1c**, while not in molecule **6.1**. As is well known, the  $\pi$ -stacking in films plays a vital role in energy and charge transport. While rapid excimer formation usually comes with

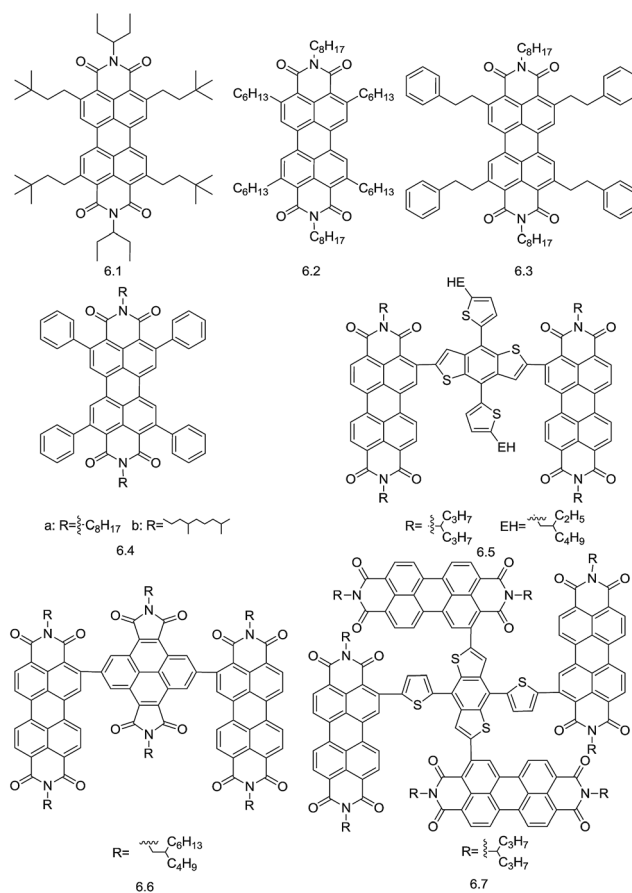


Fig. 6 Acceptors substituted *via ortho* positions.

H-aggregates,<sup>124</sup> J-aggregation prevents the necessary coupling for excimer formation and preserves good  $\pi$ -stacking for charge transport. A maximum diffusion length of 96 nm has been found in J-aggregates for PDI derivatives, which is much larger than that in disordered materials.<sup>125</sup> Patrick E. Hartnett *et al.* reported a set of *ortho* substituted PDI monomers, molecule **6.2**, molecule **6.3**, and molecule **6.4a** (in Fig. 6).<sup>126</sup> These molecules were shown to organize in slip-tacked structures, namely J-aggregation with increasing slip angles, while PDI monomers without substitution at *ortho* positions self-assembled in H-aggregation. As the slip angles increased, the electron mobility of these *ortho* substituted PDIs in TFT devices under ambient conditions increased too. The values of electron mobility were  $1.0 \times 10^{-4} \text{ cm}^2 \text{ V}^{-1} \text{ s}^{-1}$  for molecule **6.2**,  $4.2 \times 10^{-4} \text{ cm}^2 \text{ V}^{-1} \text{ s}^{-1}$  for molecule **6.3**, and  $2.4 \times 10^{-3} \text{ cm}^2 \text{ V}^{-1} \text{ s}^{-1}$  for molecule **6.4a** (as shown in Table 1). When they were paired with PBTI3T, PCEs of 0.65%, 1.2% and 3.67% were achieved based on molecules **6.2**, **6.3** and **6.4a**, respectively, following the trend of electron mobility. Molecule **6.4a** showed the smallest crystalline grains with a size around 2–5 nm. Its singlet exciton lifetime was around 200 ps, significantly longer than that in most PDI films where excimers form rapidly. Patrick E. Hartnett and co-workers later reported that the packing geometries of the *ortho*-substituted molecule **6.4b** (in Fig. 6) can be manipulated by modulating the content of solvent additives (DIO).<sup>127</sup> At a low concentration of DIO (<0.5 v%), the crystal motif organization in the slip-stacked structure

is dominant. As the DIO concentration increased (>0.5 v%), the herringbone structure appeared. When the DIO concentration was 0.5 v%, the PDI purely slip-stacked in domains and the best PCE of 3.62% was achieved based on PBDTT-FTTE:molecule **6.4b** blends. It was indicated by the photoluminescence (PL) quenching experiments that both molecular packing motifs underwent rapid charge transfer and it is even more rapid in the herringbone structure, while faster geminate recombination was observed in the herringbone structure. The acceptor with the herringbone structure exhibits stronger interaction with the polymer donor than that with the slip-stacked structure, whereas it is demonstrated that a larger D/A separation distance is beneficial for charge separation. Increased steric bulk at the D/A interface might decrease the Coulomb binding strength, thereby facilitating charge separation.<sup>128</sup> Besides, diminished coupling between adjacent PDI chromophores in the herringbone structure stimulates formation of coulombically trapped charge transfer states.<sup>129</sup> *ortho*-Substituted PDI can also be used to construct dimers, and they were verified to outperform bay-linked dimers. Donglin Zhao and co-workers linked two PDI units with a BDT unit and a pyrene diimide (PDI) unit *via* the *ortho*-position, as shown in Fig. 6.<sup>81</sup> Paired with PTB7-Th, an average PCE value of 4.76% was measured with a  $J_{sc}$  of 12.74 mA cm<sup>-2</sup>, a  $V_{oc}$  of 0.81 V, an FF of 46% and electron mobility of  $8.00 \times 10^{-4}$  cm<sup>2</sup> V<sup>-1</sup> s<sup>-1</sup> based on *ortho*-linked molecule **6.5**, while an average PCE of only 3.49% was reported for the PTB7-Th:molecule **3.6** with a  $V_{oc}$  of 0.81 V, a  $J_{sc}$  of 9.8 mA cm<sup>-2</sup>, and an FF of 44% with electron mobility of  $4.81 \times 10^{-4}$  cm<sup>2</sup> V<sup>-1</sup> s<sup>-1</sup>. The difference can also be found in the contrast between molecule **6.6** and bay-linked PDI dimer by the PDI unit. The torsion angle of the two naphthalimide planes in the PDI core was 2.0° in molecule **6.5**, and 20.2° in molecule **3.6**. However, the dihedral angle between the linker and PDI core in molecule **6.5** was 45.96°, similar to 47.79° in molecule **3.6**. Hence, the blend films showed similar morphology. The domains of molecule **6.5** showed enhanced intermolecular  $\pi$ - $\pi$  interaction and solid order, which facilitates charge transport. It accounts for the different electron mobilities. Qinghe Wu *et al.* synthesized a quasi-3D molecule **6.7** (in Fig. 6) with cross-like geometry.<sup>130</sup> A maximum PCE of 8.47% was achieved based on PTB7-Th:molecule **6.7** with a  $V_{oc}$  of 0.79 V, a  $J_{sc}$  of 17.9 mA cm<sup>-2</sup>, and an FF of 58%. Interestingly, with its unique molecular geometry, only one of the four PDI units in molecule **6.7** can have optimized  $\pi$ - $\pi$  interaction with the polymer donors due to the steric effect. When charge transfer takes place at the D/A interface, the electron can transmit to other PDI units which are farther away from the donor polymer. The electron-hole binding energy between the polymer donor and acceptor reduced due to the longer distance. It opens a new avenue to manipulate the interaction between acceptors and polymer donors, which has great effects on charge separation.

## 5. Fused PDI

It was reported that  $\pi$ -extension of the PDI core can increase the packing order and anion delocalization in the solid state. Besides, it facilitates exciton diffusion. Thus, it enhances charge mobility and facilitates charge separation. Additionally, the

spectral coverage is broadened and the energy levels are modified at the same time.<sup>131-133</sup> It indicates that fused PDI with enforced rigidity is a promising generation of electron acceptors in OSC devices. Molecules such as molecule **7.1**, with  $\pi$ -extension on the PDI core along the molecular axis (as described in Fig. 7), are widely applied as NIR dyes.<sup>134</sup>  $\pi$ -Extension of the PDI core along the equatorial axis is more investigated to design electron acceptors in OSCs.

Yu Zhong *et al.* reported a series of helical conjugated PDI oligomers bridged by double-carbon bonds, molecules **7.2a-7.2c** (in Fig. 7).<sup>135,136</sup> A PCE of 6.05% was achieved based on PBDTT-TT:molecule **7.2a**, with a  $J_{sc}$  of 13.3 mA cm<sup>-2</sup>, a  $V_{oc}$  of 0.803 V, and an FF of 56.6%. Blended with PTB7-Th, a PCE of 7.9% was reported based on molecule **7.2b** with a  $J_{sc}$  of 14.5 mA cm<sup>-2</sup>, a  $V_{oc}$  of 0.81 V, and an FF of 67% and an outstanding PCE of 8.27% was obtained using molecule **7.2c** as the acceptor with a  $J_{sc}$  of 15.1 mA cm<sup>-2</sup>, a  $V_{oc}$  of 0.81 V, and an FF of 68.2%. The high performance might be attributed to their special motifs of a mesh-like network in the solid state. It was characterized by AFM that an interpenetrating network formed in the blend film, which enabled ultrafast spatial charge separation. It indicated that ring fusion of the  $\pi$ -system was an effective approach to develop acceptors. Patrick E. Hartnett and co-workers reported a series of bay-linked PDI dimers, planar fused PDI molecule **7.3** (in Fig. 7) and nonplanar fused PDI molecule **7.4** (in Fig. 7).<sup>40</sup> They found that generally nonplanar fused PDI showed better performance than bay-linked PDI dimers and planar fused PDI. For example, when paired with PBDTT-FTTE, nonplanar fused molecule **7.4** (in Fig. 7) exhibited a PCE of 3.89% with a  $J_{sc}$  of 7.68 mA cm<sup>-2</sup>, a  $V_{oc}$  of 0.93 V, and an FF of 54.3%, while planar fused molecule **7.3** (in Fig. 7) exhibited a PCE of 0.23% with a  $J_{sc}$  of 1.51 mA cm<sup>-2</sup>, a  $V_{oc}$  of 0.89 V, and an FF of 29.3% and bay-linked PDI molecule **3.7a** (in Fig. 3) exhibited a PCE of 2.19% with a  $J_{sc}$  of 5.50 mA cm<sup>-2</sup>, a  $V_{oc}$  of 0.91 V, and an FF of 41.3%. Since all of the devices did not show large acceptor domains, the difference in performance might be ascribed to the fact that planar fused PDI interacted with polymer donors too tightly, which facilitated the formation of trapped CT states, and thus increased geminate recombination loss. Hongliang Zhong *et al.* reported a series of nonplanar fused PDI derivatives, molecules **7.5a-7.5c** (in Fig. 7) which were fused with heterocycles.<sup>41</sup> The dihedral angle between two PDI units increased as the atom size of O, S, and Se increased. The values were 15.8°, 24.4°, and 27.2°, respectively. It indicated a tunable geometry structure of fused PDI. The dihedral angles between the PDI planes played a critical role in molecular packing. Molecule **7.5b** with modest twist angles had the best packing order. The electron mobility of molecules **7.5a-7.5c** was estimated to be  $3.17 \times 10^{-7}$  cm<sup>2</sup> V<sup>-1</sup> s<sup>-1</sup>,  $1.63 \times 10^{-4}$  cm<sup>2</sup> V<sup>-1</sup> s<sup>-1</sup> and  $1.21 \times 10^{-4}$  cm<sup>2</sup> V<sup>-1</sup> s<sup>-1</sup> respectively. The device efficiency decreased following the trend of electron mobility. When they were blended with PTB7-Th, a maximum PCE of 6.72% was achieved based on molecule **7.5b** with a  $V_{oc}$  of 0.94 V, a  $J_{sc}$  of 12.48 mA cm<sup>-2</sup>, and an FF of 58.0%, while a maximum PCE of 5.77% was achieved based on molecule **7.5c** with a  $V_{oc}$  of 0.92 V, a  $J_{sc}$  of 11.19 mA cm<sup>-2</sup> and an FF of 55.0%, and a maximum PCE of 3.29% was achieved based on molecule **7.5a** with a  $V_{oc}$  of 0.92 V, a  $J_{sc}$  of 8.71 mA cm<sup>-2</sup> and an FF

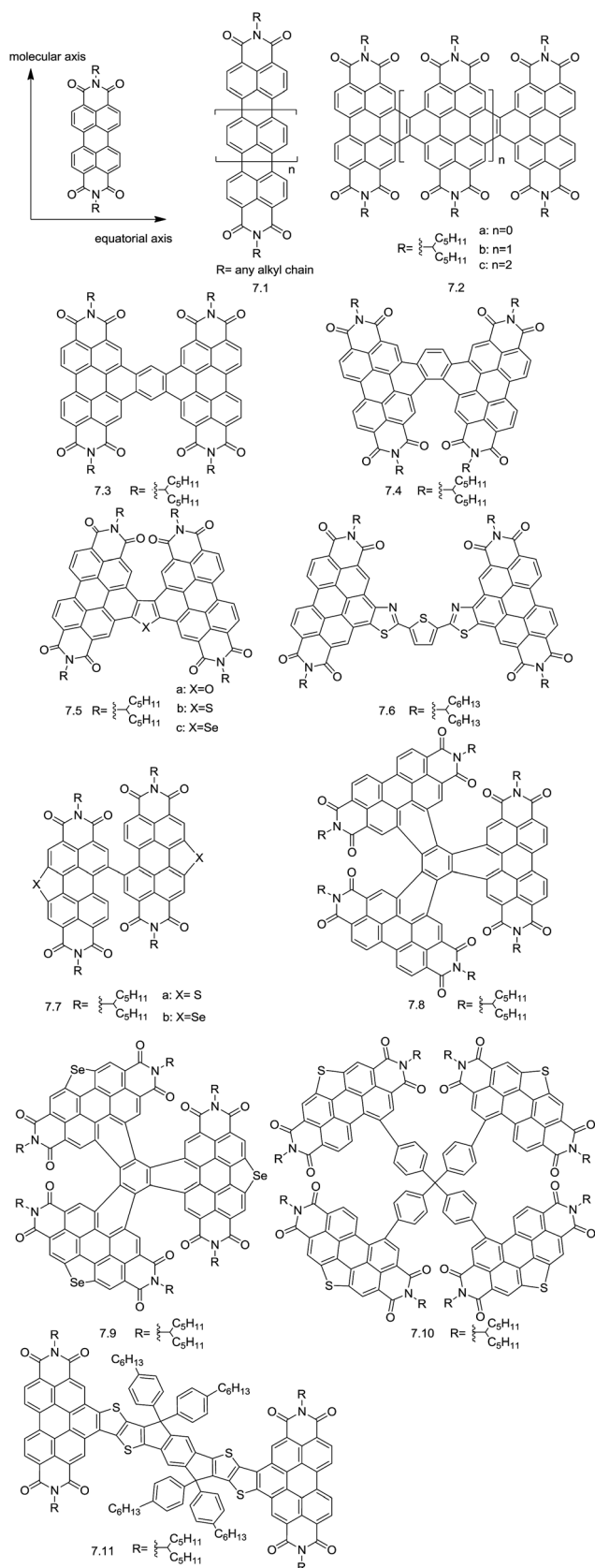


Fig. 7 Acceptors based on fused PDI.

of 40.0%. Qinqin Shi *et al.* synthesized molecule 7.6 through a novel method of iodination reaction.<sup>137</sup> A maximum PCE of 4.7% was achieved in devices based on PBDTT-F-TT:molecule 7.6 blends with a  $V_{oc}$  of 0.94 V, a  $J_{sc}$  of 9.74 mA cm<sup>-2</sup>, and an FF of 49.6%. Dan Sun *et al.* extended the molecule 3.1a with two thiophene units along the equatorial axis and obtained a new acceptor, molecule 7.7a (in Fig. 7).<sup>138</sup> The device performance improved incredibly. An excellent PCE of 7.16% was achieved in the PDBT-T1:molecule 7.7a blend, which was much higher than the highest reported PCE of molecule 3.1a, 5.9%. The values of  $J_{sc}$ ,  $V_{oc}$ , and FF were 11.65 mA cm<sup>-2</sup>, 0.90 V, and 65.5%, respectively. The electron mobility of PDBT-T1:molecule 7.7a blends was estimated to be  $3.2 \times 10^{-3}$  cm<sup>2</sup> V<sup>-1</sup> s<sup>-1</sup>, which was relatively high and balanced with the hole mobility ( $\mu_h/\mu_e = 2.3$ ). It is the high and balanced carrier mobility that accounts for the outstanding device performance. When molecule 7.7a was blended with a selenium-containing polymer donor, PBDS-Se, a higher PCE of 8.22%, with a  $J_{sc}$  of 12.90 mA cm<sup>-2</sup>,  $V_{oc}$  of 0.91 V, and FF of 70.0% was achieved.<sup>139</sup> When the S atom of molecule 7.7a was replaced by Se atom (as shown in Fig. 7), a higher PCE of 8.47% can be achieved with  $J_{sc}$  of 12.75 mA cm<sup>-2</sup>,  $V_{oc}$  of 0.91 V, and FF of 73.1% in devices based on the PDBT-T1:molecule 7.7b blend.<sup>140</sup> Notably, the value of FF was unprecedentedly high in polymer-nonfullerene BHJ OSCs. The hole mobility and electron mobility were  $3.6 \times 10^{-3}$  cm<sup>2</sup> V<sup>-1</sup> s<sup>-1</sup> and  $4.8 \times 10^{-3}$  cm<sup>2</sup> V<sup>-1</sup> s<sup>-1</sup>, respectively. The better performance of molecule 7.7b than molecule 7.7a can be ascribed to more balanced charge mobility and higher FF. Unlike conditions in molecule 7.5c, molecule 7.7b showed improved interactions between Se-Se atoms compared to that in molecule 7.7a, because the selenium atom has a bigger outermost electron cloud than sulfur. Thus, molecule 7.7b exhibited enhanced charge carrier mobility. Dong Meng *et al.* synthesized two novel acceptors, molecules 7.8 and 7.9 (in Fig. 7).<sup>141</sup> They displayed a twisted three-bladed propeller configuration with a compact 3D network in which PDI moieties in one molecule had strong  $\pi$ - $\pi$  intermolecular interactions with PDI moieties in neighbouring molecules. Molecule 7.9 showed a more compact network due to Se-O interactions and it was arranged in a slipped 3D stacking structure. These compact 3D networks were favourable for electron transport. They showed high electron mobility in the blends paired with PDBT-T1, which was  $1.0 \times 10^{-3}$  cm<sup>2</sup> V<sup>-1</sup> s<sup>-1</sup> for molecule 7.8 and  $2.2 \times 10^{-3}$  cm<sup>2</sup> V<sup>-1</sup> s<sup>-1</sup> for molecule 7.9. In consequence, devices based on molecules 7.8 and 7.9 exhibited high PCE of 8.28% and 9.28%, respectively. Wei Fan and co-workers synthesized molecule 7.10 which integrated thiophene annulation in the bay region.<sup>142</sup> The combined properties of appropriate LUMO levels, balanced carrier mobility and favourable phase separation in the BHJ films make the organic solar cell based on acceptor 7.10 show a much higher PCE of 6.2% in comparison with acceptor 4.5a based solar cells with PCE of 3.6%, which is mainly due to higher  $J_{sc}$  and FF as listed in Table 1. Shuixing Li and co-workers designed and synthesized molecule 7.11 with a fully fused backbone in which two PDI units were fused with an indacenodithieno[3,2-*b*]thiophene (IDTT) core.<sup>143</sup> Owing to the electron-donating property of IDTT, molecule 7.11



introduced. Since low LUMO offsets proved to be sufficient for charge separation, novel high efficiency acceptors with low energy loss are anticipated. (3) Light absorption. Generation of sufficient photoexcitons depends on strong light absorption complementary to polymer donors. Usually, PDI derivatives linked *via* bay positions exhibit strong absorption in the visible region of 400–600 nm and it can be extended by introducing electron-donating groups, such as BDT, TPA and oligothiophene units. Highly efficient acceptors with broad absorption band are still scarce.

To achieve high efficiency of devices based on PDI, it is necessary to modulate the photoelectric properties of PDI while maintaining relatively small aggregation size with optimized packing motifs by employing the methods demonstrated above. Constructing PDI dimers is the most used approach due to synthetic accessibility. It can be achieved by linking two PDI units with variable bridges *via* bay positions, imide positions or *ortho* positions. Constructing multidimensional PDIs enables multidimensional charge transport and separation. These molecules exhibit a compact configuration which is favourable for energy and charge transfer from a PDI moiety to another moiety in one molecule. The optical, electronic, morphological and photovoltaic properties of PDI dimers and multidimensional PDIs are closely related to the length, size, geometry, intrinsic photoelectric properties and substituting positions of linkage units. As for fused PDI molecules, the nature can be modulated by planarity, axis direction and the extent of  $\pi$ -extension. As efforts are made to judiciously design novel organic acceptors, more efforts should be devoted to explore new packing motifs of PDI in the solid state in the future. At the same time, much more efforts should be made to understand the relationships between the molecular structure, electronic properties, materials microstructure, and photoelectric performances further. Additionally, the performance of the OSCs based on non-fullerene acceptors can be further improved by selecting or designing suitable donor materials, developing appropriate film-processing methods, and engineering the interfaces between the photoactive layer and electrodes.

## Acknowledgements

This work was financially supported by the Applied Basic Research Programs of Wuhan (No. 2015010101010018), the State Key Laboratory of Luminescent Materials and Devices (South China University of Technology) (2016-skllmd-02), Wuhan Yellow Crane Program for Excellent Talents and Hubei Technology Innovation Major Project.

## References

- 1 J. Roncali, *Acc. Chem. Res.*, 2009, **42**, 1719–1730.
- 2 Y. Liu, J. Liu, L. Zhang, J. Fang, W. Zhang and Z. Liu, *Chin. J. Chem.*, 2014, 1021–1033.
- 3 C. Li, M. Liu, N. G. Pschirer, M. Baumgarten and K. Müllen, *Chem. Rev.*, 2010, **110**, 6817–6855.
- 4 Y. Lin and X. Zhan, *Adv. Energy Mater.*, 2015, **5**, 1501063.
- 5 A. Facchetti, *Mater. Today*, 2013, **16**, 123–132.
- 6 S. B. Darling and F. You, *RSC Adv.*, 2013, **3**, 17633–17648.
- 7 A. J. Heeger, *Adv. Mater.*, 2014, **26**, 10–28.
- 8 Y. Li, *Acc. Chem. Res.*, 2012, **45**, 723–733.
- 9 Y. Lin and X. Zhan, *Acc. Chem. Res.*, 2016, **49**, 175–183.
- 10 L. Ye, S. Zhang, L. Huo, M. Zhang and J. Hou, *Acc. Chem. Res.*, 2014, **47**, 1595–1603.
- 11 M. C. Scharber and N. S. Sariciftci, *Prog. Polym. Sci.*, 2013, **38**, 1929–1940.
- 12 C. Zhan, X. Zhang and J. Yao, *RSC Adv.*, 2015, **5**, 93002–93026.
- 13 J. Song and Z. Bo, in *Organic and Hybrid Solar Cells*, ed. H. Huang and J. Huang, Springer International Publishing, Cham, 2014, pp. 53–96.
- 14 B. C. Thompson and J. M. J. Frechet, *ChemInform*, 2008, **39**, 58–77.
- 15 P. Sonar, J. P. F. Lim and K. L. Chan, *Energy Environ. Sci.*, 2011, **4**, 1558–1574.
- 16 L. Gao, Z.-G. Zhang, H. Bin, L. Xue, Y. Yang, C. Wang, F. Liu, T. P. Russell and Y. Li, *Adv. Mater.*, 2016, **28**, 8288–8295.
- 17 Y. Lin and X. Zhan, *Mater. Horiz.*, 2014, **1**, 470–488.
- 18 H. Li, T. Earmme, G. Ren, A. Saeki, S. Yoshikawa, N. M. Murari, S. Subramaniam, M. J. Crane, S. Seki and S. A. Jenekhe, *J. Am. Chem. Soc.*, 2014, **136**, 14589–14597.
- 19 J. Liu, S. Chen, D. Qian, B. Gautam, G. Yang, J. Zhao, J. Bergqvist, F. Zhang, W. Ma, H. Ade, O. Inganäs, K. Gundogdu, F. Gao and H. Yan, *Nat. Energy*, 2016, **1**, 16089.
- 20 W. Liu, S. Li, J. Huang, S. Yang, J. Chen, L. Zuo, M. Shi, X. Zhan, C.-Z. Li and H. Chen, *Adv. Mater.*, 2016, DOI: 10.1002/adma.201603518.
- 21 W. Zhao, D. Qian, S. Zhang, S. Li, O. Inganäs, F. Gao and J. Hou, *Adv. Mater.*, 2016, **28**, 4734–4739.
- 22 Y. Lin, Q. He, F. Zhao, L. Huo, J. Mai, X. Lu, C.-J. Su, T. Li, J. Wang, J. Zhu, Y. Sun, C. Wang and X. Zhan, *J. Am. Chem. Soc.*, 2016, **138**, 2973–2976.
- 23 S. Li, L. Ye, W. Zhao, S. Zhang, S. Mukherjee, H. Ade and J. Hou, *Adv. Mater.*, 2016, DOI: 10.1002/adma.201602776.
- 24 Y. Wu, H. Bai, Z. Wang, P. Cheng, S. Zhu, Y. Wang, W. Ma and X. Zhan, *Energy Environ. Sci.*, 2015, **8**, 3215–3221.
- 25 Y. Lin, Z.-G. Zhang, H. Bai, J. Wang, Y. Yao, Y. Li, D. Zhu and X. Zhan, *Energy Environ. Sci.*, 2015, **8**, 610–616.
- 26 Y. Lin, F. Zhao, Q. He, L. Huo, Y. Wu, T. C. Parker, W. Ma, Y. Sun, C. Wang, D. Zhu, A. J. Heeger, S. R. Marder and X. Zhan, *J. Am. Chem. Soc.*, 2016, **138**, 4955–4961.
- 27 Y. Lin, J. Wang, Z.-G. Zhang, H. Bai, Y. Li, D. Zhu and X. Zhan, *Adv. Mater.*, 2015, **27**, 1170–1174.
- 28 Y. Lin, T. Li, F. Zhao, L. Han, Z. Wang, Y. Wu, Q. He, J. Wang, L. Huo, Y. Sun, C. Wang, W. Ma and X. Zhan, *Adv. Energy Mater.*, 2016, **6**, 1600854.
- 29 X. Zhan, Z. a. Tan, B. Domercq, Z. An, X. Zhang, S. Barlow, Y. Li, D. Zhu, B. Kippelen and S. R. Marder, *J. Am. Chem. Soc.*, 2007, **129**, 7246–7247.
- 30 F. Fernandez-Lazaro, N. Zink-Lorre and A. Sastre-Santos, *J. Mater. Chem. A*, 2016, **4**, 9336–9346.
- 31 C. Zhan and J. Yao, *Chem. Mater.*, 2016, **28**, 1948–1964.
- 32 C. Li and H. Wonneberger, *Adv. Mater.*, 2012, **24**, 613–636.

- 33 S. M. McAfee, J. M. Topple, I. G. Hill and G. C. Welch, *J. Mater. Chem. A*, 2015, **3**, 16393–16408.
- 34 C. B. Nielsen, S. Holliday, H.-Y. Chen, S. J. Cryer and I. McCulloch, *Acc. Chem. Res.*, 2015, **48**, 2803–2812.
- 35 D. M. Stoltzfus, J. E. Donaghey, A. Armin, P. E. Shaw, P. L. Burn and P. Meredith, *Chem. Rev.*, 2016, DOI: 10.1021/acs.chemrev.6b00126.
- 36 P. E. Keivanidis, I. A. Howard and R. H. Friend, *Adv. Funct. Mater.*, 2008, **18**, 3189–3202.
- 37 A. Pivrikas, N. S. Sariciftci, G. Juška and R. Österbacka, *Prog. Photovolt: Res. Appl.*, 2007, **15**, 677–696.
- 38 M. Stolterfoht, A. Armin, S. Shoaee, I. Kassal, P. Burn and P. Meredith, *Nat. Commun.*, 2016, **7**, DOI: 10.1038/ncomms11944.
- 39 A. D. Hendsbee, S. M. McAfee, J.-P. Sun, T. M. McCormick, I. G. Hill and G. C. Welch, *J. Mater. Chem. C*, 2015, **3**, 8904–8915.
- 40 P. E. Hartnett, H. S. S. R. Matte, N. D. Eastham, N. E. Jackson, Y. Wu, L. X. Chen, M. A. Ratner, R. P. H. Chang, M. C. Hersam, M. R. Wasielewski and T. J. Marks, *Chem. Sci.*, 2016, **7**, 3543–3555.
- 41 H. Zhong, C.-H. Wu, C.-Z. Li, J. Carpenter, C.-C. Chueh, J.-Y. Chen, H. Ade and A. K. Y. Jen, *Adv. Mater.*, 2016, **28**, 951–958.
- 42 X. Zhang, B. Jiang, X. Zhang, A. Tang, J. Huang, C. Zhan and J. Yao, *J. Phys. Chem. C*, 2014, **118**, 24212–24220.
- 43 Y. Cai, L. Huo, X. Sun, D. Wei, M. Tang and Y. Sun, *Adv. Energy Mater.*, 2015, **5**, 1500032.
- 44 R. K. Dubey, A. Efimov and H. Lemmetyinen, *Chem. Mater.*, 2011, **23**, 778–788.
- 45 J. Yi, J. Wang, Y. Lin, W. Gao, Y. Ma, H. Tan, H. Wang and C.-Q. Ma, *Dyes Pigm.*, 2017, **136**, 335–346.
- 46 J. Yi, Y. Ma, J. Dou, Y. Lin, Y. Wang, C.-Q. Ma and H. Wang, *Dyes Pigm.*, 2016, **126**, 86–95.
- 47 W. Jiang, L. Ye, X. Li, C. Xiao, F. Tan, W. Zhao, J. Hou and Z. Wang, *Chem. Commun.*, 2013, **50**, 1024–1026.
- 48 L. Ye, W. Jiang, W. Zhao, S. Zhang, D. Qian, Z. Wang and J. Hou, *Small*, 2014, **10**, 4658–4663.
- 49 Y. Zang, C.-Z. Li, C.-C. Chueh, S. T. Williams, W. Jiang, Z.-H. Wang, J.-S. Yu and A. K. Y. Jen, *Adv. Mater.*, 2014, **26**, 5708–5714.
- 50 L. Ye, W. Jiang, W. Zhao, S. Zhang, Y. Cui, Z. Wang and J. Hou, *Org. Electron.*, 2014, **17**, 295–303.
- 51 L. Ye, K. Sun, W. Jiang, S. Zhang, W. Zhao, H. Yao, Z. Wang and J. Hou, *ACS Appl. Mater. Interfaces*, 2015, **7**, 9274–9280.
- 52 G. Feng, Y. Xu, J. Zhang, Z. Wang, Y. Zhou, Y. Li, Z. Wei, C. Li and W. Li, *J. Mater. Chem. A*, 2016, **4**, 6056–6063.
- 53 C.-H. Wu, C.-C. Chueh, Y.-Y. Xi, H.-L. Zhong, G.-P. Gao, Z.-H. Wang, L. D. Pozzo, T.-C. Wen and A. K. Y. Jen, *Adv. Funct. Mater.*, 2015, **25**, 5326–5332.
- 54 M. C. Scharber, D. Mühlbacher, M. Koppe, P. Denk, C. Waldauf, A. J. Heeger and C. J. Brabec, *Adv. Mater.*, 2006, **18**, 789–794.
- 55 H.-Y. Chen, J. Hou, S. Zhang, Y. Liang, G. Yang, Y. Yang, L. Yu, Y. Wu and G. Li, *Nat. Photonics*, 2009, **3**, 649–653.
- 56 G. Li, C.-W. Chu, V. Shrotriya, J. Huang and Y. Yang, *Appl. Phys. Lett.*, 2006, **88**, 253503.
- 57 Z. Lu, B. Jiang, X. Zhang, A. Tang, L. Chen, C. Zhan and J. Yao, *Chem. Mater.*, 2014, **26**, 2907–2914.
- 58 Y. Yu, F. Yang, Y. Ji, Y. Wu, A. Zhang, C. Li and W. Li, *J. Mater. Chem. C*, 2016, **4**, 4134–4137.
- 59 W. Li, K. H. Hendriks, A. Furlan, M. M. Wienk and R. A. J. Janssen, *J. Am. Chem. Soc.*, 2015, **137**, 2231–2234.
- 60 X. Zhang, Z. Lu, L. Ye, C. Zhan, J. Hou, S. Zhang, B. Jiang, Y. Zhao, J. Huang, S. Zhang, Y. Liu, Q. Shi, Y. Liu and J. Yao, *Adv. Mater.*, 2013, **25**, 5791–5797.
- 61 Y. Chen, A. Tang, X. Zhang, Z. Lu, J. Huang, C. Zhan and J. Yao, *J. Mater. Chem. A*, 2014, **2**, 1869–1876.
- 62 J. Huang, X. Wang, X. Zhang, Z. Niu, Z. Lu, B. Jiang, Y. Sun, C. Zhan and J. Yao, *ACS Appl. Mater. Interfaces*, 2014, **6**, 3853–3862.
- 63 J. Wang, Y. Yao, S. Dai, X. Zhang, W. Wang, Q. He, L. Han, Y. Lin and X. Zhan, *J. Mater. Chem. A*, 2015, **3**, 13000–13010.
- 64 X. Zhang, C. Zhan and J. Yao, *Chem. Mater.*, 2015, **27**, 166–173.
- 65 X. Zhang, W. Li, J. Yao and C. Zhan, *ACS Appl. Mater. Interfaces*, 2016, **8**, 15415–15421.
- 66 B. Jiang, X. Zhang, Y. Zheng, G. Yu, J. Yao and C. Zhan, *RSC Adv.*, 2016, **6**, 43715–43718.
- 67 Y. Chen, A. Tang, X. Zhang, Z. Lu, J. Huang, C. Zhan and J. Yao, *J. Mater. Chem. A*, 2014, **2**, 1869–1876.
- 68 Y. Chen, X. Zhang, C. Zhan and J. Yao, *ACS Appl. Mater. Interfaces*, 2015, **7**, 6462–6471.
- 69 Y. Chen, C. Zhan and J. Yao, *Chem.-Asian J.*, 2016, **11**, 2620–2632.
- 70 A. Sharenko, C. M. Proctor, T. S. van der Poll, Z. B. Henson, T.-Q. Nguyen and G. C. Bazan, *Adv. Mater.*, 2013, **25**, 4403–4406.
- 71 R. Singh, E. Aluicio-Sarduy, Z. Kan, T. Ye, R. C. I. Mackenzie and P. E. Keivanidis, *J. Mater. Chem. A*, 2014, **2**, 14348–14353.
- 72 G. Ren, E. Ahmed and S. A. Jenekhe, *Adv. Energy Mater.*, 2011, **1**, 946–953.
- 73 Z. Lu, X. Zhang, C. Zhan, B. Jiang, X. Zhang, L. Chen and J. Yao, *Phys. Chem. Chem. Phys.*, 2013, **15**, 11375–11385.
- 74 X. Zhang, J. Yao and C. Zhan, *Sci. China:Chem.*, 2016, **59**, 209–217.
- 75 W. T. Hadmojo, S. Y. Nam, T. J. Shin, S. C. Yoon, S.-Y. Jang and I. H. Jung, *J. Mater. Chem. A*, 2016, **4**, 12308–12318.
- 76 J.-F. Jheng, Y.-Y. Lai, J.-S. Wu, Y.-H. Chao, C.-L. Wang and C.-S. Hsu, *Adv. Mater.*, 2013, **25**, 2445–2451.
- 77 N. E. Jackson, B. M. Savoie, K. L. Kohlstedt, M. Olvera de la Cruz, G. C. Schatz, L. X. Chen and M. A. Ratner, *J. Am. Chem. Soc.*, 2013, **135**, 10475–10483.
- 78 J. Zhao, Y. Li, J. Zhang, L. Zhang, J. Y. L. Lai, K. Jiang, C. Mu, Z. Li, C. L. C. Chan, A. Hunt, S. Mukherjee, H. Ade, X. Huang and H. Yan, *J. Mater. Chem. A*, 2015, **3**, 20108–20112.
- 79 X. Zhang, J. Yao and C. Zhan, *Chem. Commun.*, 2015, **51**, 1058–1061.
- 80 B. Jiang, X. Zhang, C. Zhan, Z. Lu, J. Huang, X. Ding, S. He and J. Yao, *Polym. Chem.*, 2013, **4**, 4631–4638.
- 81 D. Zhao, Q. Wu, Z. Cai, T. Zheng, W. Chen, J. Lu and L. Yu, *Chem. Mater.*, 2016, **28**, 1139–1146.

- 82 Q. Yan, Y. Zhou, Y.-Q. Zheng, J. Pei and D. Zhao, *Chem. Sci.*, 2013, **4**, 4389–4394.
- 83 Y. Liu, C. Mu, K. Jiang, J. Zhao, Y. Li, L. Zhang, Z. Li, J. Y. L. Lai, H. Hu, T. Ma, R. Hu, D. Yu, X. Huang, B. Z. Tang and H. Yan, *Adv. Mater.*, 2015, **27**, 1014.
- 84 J. Zhao, Y. Li, H. Lin, Y. Liu, K. Jiang, C. Mu, T. Ma, J. Y. Lin Lai, H. Hu, D. Yu and H. Yan, *Energy Environ. Sci.*, 2015, **8**, 520–525.
- 85 L. Yang, Y. Chen, S. Chen, T. Dong, W. Deng, L. Lv, S. Yang, H. Yan and H. Huang, *J. Power Sources*, 2016, **324**, 538–546.
- 86 Y. Lin, J. Wang, S. Dai, Y. Li, D. Zhu and X. Zhan, *Adv. Energy Mater.*, 2014, **4**, 1400402.
- 87 G. E. Park, H. J. Kim, S. Choi, D. H. Lee, M. A. Uddin, H. Y. Woo, M. J. Cho and D. H. Choi, *Chem. Commun.*, 2016, **52**, 8873–8876.
- 88 J. Yi, Y. Wang, Q. Luo, Y. Lin, H. Tan, H. Wang and C.-Q. Ma, *Chem. Commun.*, 2016, **52**, 1649–1652.
- 89 X.-F. Wu, W.-F. Fu, Z. Xu, M. Shi, F. Liu, H.-Z. Chen, J.-H. Wan and T. P. Russell, *Adv. Funct. Mater.*, 2015, **25**, 5954–5966.
- 90 S. Dai, Y. Lin, P. Cheng, Y. Wang, X. Zhao, Q. Ling and X. Zhan, *Dyes Pigm.*, 2015, **114**, 283–289.
- 91 Y. Lin, Y. Wang, J. Wang, J. Hou, Y. Li, D. Zhu and X. Zhan, *Adv. Mater.*, 2014, **26**, 5137–5142.
- 92 Z. Hu, X.-d. Li, W. Zhang, A. Liang, D. Ye, Z. Liu, J. Liu, Y. Liu and J. Fang, *RSC Adv.*, 2014, **4**, 5591–5597.
- 93 Z. Liu, L. Zhang, X. Gao, L. Zhang, Q. Zhang and J. Chen, *Dyes Pigm.*, 2016, **127**, 155–160.
- 94 Q. Wu, L. Li, J. Hai, X. Zhang, Z. Lu, J. Yang, Y. Liu, L. Zhang and C. Zhan, *Dyes Pigm.*, 2016, **132**, 41–47.
- 95 S. Li, W. Liu, C.-Z. Li, F. Liu, Y. Zhang, M. Shi, H. Chen and T. P. Russell, *J. Mater. Chem. A*, 2016, **4**, 10659–10665.
- 96 J. Lee, R. Singh, D. H. Sin, H. G. Kim, K. C. Song and K. Cho, *Adv. Mater.*, 2016, **28**, 69–76.
- 97 S.-Y. Liu, C.-H. Wu, C.-Z. Li, S.-Q. Liu, K.-H. Wei, H.-Z. Chen and A. K. Y. Jen, *Adv. Sci.*, 2015, **2**, 1500014.
- 98 Y. Liu, J. Y. L. Lai, S. Chen, Y. Li, K. Jiang, J. Zhao, Z. Li, H. Hu, T. Ma, H. Lin, J. Liu, J. Zhang, F. Huang, D. Yu and H. Yan, *J. Mater. Chem. A*, 2015, **3**, 13632–13636.
- 99 H. Lin, S. Chen, H. Hu, L. Zhang, T. Ma, J. Y. L. Lai, Z. Li, A. Qin, X. Huang, B. Tang and H. Yan, *Adv. Mater.*, 2016, **28**, 8546–8551.
- 100 F. G. Brunetti, X. Gong, M. Tong, A. J. Heeger and F. Wudl, *Angew. Chem., Int. Ed.*, 2010, **49**, 532–536.
- 101 Y. Fan, S. Barlow, S. Zhang, B. Lin and S. R. Marder, *RSC Adv.*, 2016, **6**, 70493–70500.
- 102 X. Zhan, A. Facchetti, S. Barlow, T. J. Marks, M. A. Ratner, M. R. Wasielewski and S. R. Marder, *Adv. Mater.*, 2011, **23**, 268–284.
- 103 C. Huang, S. Barlow and S. R. Marder, *J. Org. Chem.*, 2011, **76**, 2386–2407.
- 104 V. Kamm, G. Battagliarin, I. A. Howard, W. Pisula, A. Mavrinskiy, C. Li, K. Müllen and F. Laquai, *Adv. Energy Mater.*, 2011, **1**, 297–302.
- 105 T. Ye, R. Singh, H. Butt, G. Floudas and P. E. Keivanidis, *ACS Appl. Mater. Interfaces*, 2013, **5**, 11844–11857.
- 106 D. W. Gehrig, S. Roland, I. A. Howard, V. Kamm, H. Mangold, D. Neher and F. Laquai, *J. Phys. Chem. C*, 2014, **118**, 20077–20085.
- 107 Y. Chen, X. Zhang, C. Zhan and J. Yao, *Phys. Status Solidi*, 2015, **212**, 1961–1968.
- 108 R. Singh, R. Shivanna, A. Iosifidis, H.-J. Butt, G. Floudas, K. S. Narayan and P. E. Keivanidis, *ACS Appl. Mater. Interfaces*, 2015, **7**, 24876–24886.
- 109 S. Shoaee, F. Deledalle, P. Shakya Tuladhar, R. Shivanna, S. Rajaram, K. S. Narayan and J. R. Durrant, *J. Phys. Chem. Lett.*, 2015, **6**, 201–205.
- 110 J. Wang and Z. Liang, *ACS Appl. Mater. Interfaces*, 2016, **8**, 22418–22424.
- 111 J.-P. Sun, A. D. Hendsbee, A. J. Dobson, G. C. Welch and I. G. Hill, *Org. Electron.*, 2016, **35**, 151–157.
- 112 H. Langhals and W. Jona, *Angew. Chem., Int. Ed.*, 1998, **37**, 952–955.
- 113 S. Rajaram, R. Shivanna, S. K. Kandappa and K. S. Narayan, *J. Phys. Chem. Lett.*, 2012, **3**, 2405–2408.
- 114 N. Liang, K. Sun, Z. Zheng, H. Yao, G. Gao, X. Meng, Z. Wang, W. Ma and J. Hou, *Adv. Energy Mater.*, 2016, **6**, 1600060.
- 115 T. M. Wilson, M. J. Tauber and M. R. Wasielewski, *J. Am. Chem. Soc.*, 2009, **131**, 8952–8957.
- 116 T. M. Wilson, T. A. Zeidan, M. Hariharan, F. D. Lewis and M. R. Wasielewski, *Angew. Chem., Int. Ed.*, 2010, **49**, 2385–2388.
- 117 G. Gao, X. Zhang, D. Meng, A. Zhang, Y. Liu, W. Jiang, Y. Sun and Z. Wang, *RSC Adv.*, 2016, **6**, 14027–14033.
- 118 W. Chen, X. Yang, G. Long, X. Wan, Y. Chen and Q. Zhang, *J. Mater. Chem. C*, 2015, **3**, 4698–4705.
- 119 S. Nakazono, S. Easwaramoorthi, D. Kim, H. Shinokubo and A. Osuka, *Org. Lett.*, 2009, **11**, 5426–5429.
- 120 S. Nakazono, Y. Imazaki, H. Yoo, J. Yang, T. Sasamori, N. Tokitoh, T. Cédric, H. Kageyama, D. Kim, H. Shinokubo and A. Osuka, *Chem.–Eur. J.*, 2009, **15**, 7530–7533.
- 121 G. Battagliarin, C. Li, V. Enkelmann and K. Müllen, *Org. Lett.*, 2011, **13**, 3012–3015.
- 122 T. Teraoka, S. Hiroto and H. Shinokubo, *Org. Lett.*, 2011, **13**, 2532–2535.
- 123 J. Zhang, S. Singh, D. K. Hwang, S. Barlow, B. Kippelen and S. R. Marder, *J. Mater. Chem. C*, 2013, **1**, 5093–5100.
- 124 A. Schubert, V. Settels, W. Liu, F. Würthner, C. Meier, R. F. Fink, S. Schindlbeck, S. Lochbrunner, B. Engels and V. Engel, *J. Phys. Chem. Lett.*, 2013, **4**, 792–796.
- 125 H. Marciniak, X.-Q. Li, F. Würthner and S. Lochbrunner, *J. Phys. Chem. A*, 2011, **115**, 648–654.
- 126 P. E. Hartnett, A. Timalsina, H. S. S. R. Matte, N. Zhou, X. Guo, W. Zhao, A. Facchetti, R. P. H. Chang, M. C. Hersam, M. R. Wasielewski and T. J. Marks, *J. Am. Chem. Soc.*, 2014, **136**, 16345–16356.
- 127 P. E. Hartnett, E. A. Margulies, H. S. S. R. Matte, M. C. Hersam, T. J. Marks and M. R. Wasielewski, *Chem. Mater.*, 2016, **28**, 3928–3936.

- 128 T. W. Holcombe, J. E. Norton, J. Rivnay, C. H. Woo, L. Goris, C. Piliago, G. Griffini, A. Sellinger, J.-L. Brédas, A. Salleo and J. M. J. Fréchet, *J. Am. Chem. Soc.*, 2011, **133**, 12106–12114.
- 129 B. M. Savoie, A. Rao, A. A. Bakulin, S. Gelin, B. Movaghar, R. H. Friend, T. J. Marks and M. A. Ratner, *J. Am. Chem. Soc.*, 2014, **136**, 2876–2884.
- 130 Q. Wu, D. Zhao, A. M. Schneider, W. Chen and L. Yu, *J. Am. Chem. Soc.*, 2016, **138**, 7248–7251.
- 131 H. Qian, Z. Wang, W. Yue and D. Zhu, *J. Am. Chem. Soc.*, 2007, **129**, 10664–10665.
- 132 H. Qian, W. Yue, Y. Zhen, S. Di Motta, E. Di Donato, F. Negri, J. Qu, W. Xu, D. Zhu and Z. Wang, *J. Org. Chem.*, 2009, **74**, 6275–6282.
- 133 W. Jiang, Y. Li and Z. Wang, *Acc. Chem. Res.*, 2014, **47**, 3135–3147.
- 134 Chaolumen, H. Enno, M. Murata, A. Wakamiya and Y. Murata, *Chem.-Asian J.*, 2014, **9**, 3136–3140.
- 135 Y. Zhong, M. T. Trinh, R. Chen, W. Wang, P. P. Khlyabich, B. Kumar, Q. Xu, C.-Y. Nam, M. Y. Sfeir, C. Black, M. L. Steigerwald, Y.-L. Loo, S. Xiao, F. Ng, X. Y. Zhu and C. Nuckolls, *J. Am. Chem. Soc.*, 2014, **136**, 15215–15221.
- 136 Y. Zhong, M. T. Trinh, R. Chen, G. E. Purdum, P. P. Khlyabich, M. Sezen, S. Oh, H. Zhu, B. Fowler, B. Zhang, W. Wang, C.-Y. Nam, M. Y. Sfeir, C. T. Black, M. L. Steigerwald, Y.-L. Loo, F. Ng, X. Y. Zhu and C. Nuckolls, *Nat. Commun.*, 2015, **6**, 8242.
- 137 Q. Shi, S. Zhang, J. Zhang, V. F. Oswald, A. Amassian, S. R. Marder and S. B. Blakey, *J. Am. Chem. Soc.*, 2016, **138**, 3946–3949.
- 138 D. Sun, D. Meng, Y. Cai, B. Fan, Y. Li, W. Jiang, L. Huo, Y. Sun and Z. Wang, *J. Am. Chem. Soc.*, 2015, **137**, 11156–11162.
- 139 T. Liu, D. Meng, Y. Cai, X. Sun, Y. Li, L. Huo, F. Liu, Z. Wang, T. P. Russell and Y. Sun, *Adv. Sci.*, 2016, **3**, 1600117.
- 140 D. Meng, D. Sun, C. Zhong, T. Liu, B. Fan, L. Huo, Y. Li, W. Jiang, H. Choi, T. Kim, J. Y. Kim, Y. Sun, Z. Wang and A. J. Heeger, *J. Am. Chem. Soc.*, 2016, **138**, 375–380.
- 141 D. Meng, H. Fu, C. Xiao, X. Meng, T. Winands, W. Ma, W. Wei, B. Fan, L. Huo, N. L. Doltsinis, Y. Li, Y. Sun and Z. Wang, *J. Am. Chem. Soc.*, 2016, **138**, 10184–10190.
- 142 W. Fan, N. Liang, D. Meng, J. Feng, Y. Li, J. Hou and Z. Wang, *Chem. Commun.*, 2016, **52**, 11500–11503.
- 143 S. Li, W. Liu, C.-Z. Li, T.-K. Lau, X. Lu, M. Shi and H. Chen, *J. Mater. Chem. A*, 2016, **4**, 14983–14987.